Structures and Materials Research
Department of Civil Engineering

Report No. UCSESM 70-1

Analysis of Stiffened Plates Using the Finite Element Method

by

Pal G. Bergan
Ray W. Clough
Soheil Mojtahedi

This research was sponsored by the Department of Structural Mechanics, Naval Ship Research and Development Center under the Naval Ship Systems Command Subproject SF 013 0301, Task 1968, Contract N00014-67-A-0114-0020.

Structural Engineering Laboratory
University of California
Berkeley, California

January 1970

ABSTRACT

This report describes a finite element procedure for the analysis of plates with stiffening elements located on one side. The structure is idealized by an assemblage of quadrilateral elements simulating both membrane and plate bending actions for the plate. The stiffeners are discretized using special spar-elements with additional bar-elements simulating the top flanges.

The report includes a complete users manual for the computer program. The use of the program is demonstrated by listing of input information and output results for some cases.

Application of the method to some structures of particular interest to naval architects are discussed in Chapter 4. The cases treated are a section of a orthogonally stiffened platestrip, and infinite platestrip with transverse stiffeners, and a square plate with two orthogonal stiffeners.

The program can be used directly in design. However, based on systematic variations of the geometry of plate and stiffeners for an orthogonally stiffened plate field, it has been possible to extract maximum stress-curves based on the computer program results. These curves will hopefully be of value to the designer at an early stage in the design process.

A complete listing of the program is given in a separate Appendix.

ACKNOWLEDGMENT

This research was sponsored by the Department of Structural Mechanics, Naval Ship Research and Development Center under the Naval Ship Systems Command Subproject SF 013 0301, Task 1968, Contract N00014-67-A-0114-0020.

TABLE OF CONTENTS

1. INTRODUCTION

Stiffened plates are frequently utilized in the design of ship structures. The need for accurate methods of calculation of stresses and displacements for this type of structural system is evident because of its consequences for economy, weight and safety of the structures.

Up to the present time, the method of calculation that has been used generally to solve the local plate-stiffener interaction problem employs a series expansion of a stress function to solve the differential equations of equilibrium [19], [24]. The stress function approach has several drawbacks which limit its general applicability. In most cases, it is necessary to express the boundary conditions in terms of stresses instead of displacements. Moreover, when using this method it is almost impossible to write a general computer program that can deal with arbitrary geometry of the stiffened plate and with arbitrary boundary conditions.

Usually, the complete stress function analysis is not performed. Instead, the concepts of "shear lag" and "effective width" are often used in design, and the overall stiffened plate bending problem is solved as a grillage system or using orthotropic plate theory. For this purpose, the effective width may be obtained from tables or diagrams that are derived from stress function calculations. However, the effective width approach does not give a complete picture of the stress distribution throughout the plate, and its accuracy in case of orthogonal stiffening is questionable.

The finite element method has proven to be a powerful method of computation for many kinds of structural problems. This method has been in rapid

development since the first paper was published in 1956 [20]. Important finite element types that have been developed in the past decade include plate bending elements and membrane elements [23], [14] and [10].

An important trend in the search for new elements is the development of more specialized elements, that is, elements that are designed to represent the special form of behavior that can be anticipated in a particular type of structural part. One example of such an element is the so-called spar element. This element is most appropriate for idealizing the stiffeners on a stiffened plate system.

An extensive study of different types of elements suitable for the calculation of stiffened plates has been carried out in this investigation. This study resulted in a computer program called LASP, programmed by the first mentioned of the authors. This program will be described later in this report. LASP stands for "Linear Analysis of Stiffened Plates". The term "linear analysis" is used to emphasize that large deflection and non-linear material effects are not included. The program can be used for analysis of plates with arbitrary geometry and boundary conditions and with orthogonally oriented stiffeners on one side. A mesh-generating subroutine makes the program particularly easy to use.

Based on the experience gained from this project, the authors of this report are confident that the finite element approach is more powerful than any other available method for the analysis of stiffened plates.

2. METHOD OF ANALYSIS

2.1. Discretization of the Stiffened Plate.

The finite element method will not be discussed in detail here; good general references are available elsewhere, [23], [14] and [10]. As indicated by the name of the method, the structure is idealized as an assemblage of discrete structural elements. A set of displacement functions is assumed within each subregion (finite element). The displacement functions, usually polynomials, can be expressed by the displacements at a corresponding number of nodal points at the element boundary. Using the "displacement method" [14], the strain energy within each element can be expressed in terms of the local nodal point displacements. Adding up the strain energies for all elements, the energy for the total system is obtained. Putting the variation of the total potential equal to zero, one is left with the stiffness relation for the entire system. Examples of how the finite element idealization ought to be performed in the case of the stiffened plate system are given in Chapter 3 and Chapter 4.

The elements used here for the stiffened plate problem are of four main types. The plate itself must be divided into quadrilateral regions. For each such region (finite element) a plate bending stiffness and a membrane stiffness are evaluated. The stiffeners are divided into quadrilateral elements having membrane action only. One element only is taken over the entire height (distance perpendicular to the plate) of the stiffeners. The ends of each stiffener element are perpendicular to the main plate. The lower nodal points of the stiffener elements must coincide with nodal points of the plate, so that coupling can be established between the stiffeners and the bending and membrane

actions of the plate. Torsional stiffness of the stiffeners is not included in this analysis because it is assumed to be of negligible importance; however, it could be easily added. The top flanges of the stiffeners are idealized by bar elements having axial rigidities only. The bending stiffness of the top flange is considered to be negligible compared to the in-plane bending rigidity of the total stiffener.

A more detailed discussion of the different elements follows.

2.2. Membrane Element for the Plate.

The plane stress element is a general quadrilateral with four corner nodal points and one internal nodal point as shown in Fig. 2.1. The internal node is eliminated during the stiffness analysis by static condensation. The u and v displacements are defined by interpolation polynomials in the oblique ξ - η system. A similar type of element is described by Zienkiewicz [23]. The element stiffness is evaluated by a 4 by 4 numerical integration scheme (Gaussian quadrature).

In addition to its corner nodes, the element may have a specified number (up to 4) of midside nodes, each having one tangential degree of freedom. The corresponding displacement pattern is defined as a quadratic deviation from the linear interpolation between the tangential displacements at the two adjacent side nodes. Numerical calculations of stiffened plates have revealed that it is a great advantage to include these additional nodes where the stiffeners are connected to the plate. Instead of a constant tangential strain along the element side, a linearly varying strain is obtained by using such a node.

When this type of element is tested in a cantilever beam, however, one

easily discovers that the element is far too stiff. This is mainly due to the high shear strain energy connected with the displacement patterns assumed in the typical bending modes of the element, see Fig. 2.2. The displacement functions within the element require that the edges of the element remain straight during pure bending deformation, while in the real case, the sides would tend to be curved. An element with a modified flexural response has been proposed by Doherty, Wilson and Taylor [8]. They suggested that the shear strain energy resulting from the pure bending modes of the element should be neglected. The resulting element consequently has a constant shear stress throughout the element (*).

A comparison study was carried out to investigate the performance of the "constant shear" element in stiffened plate problems, see Section 4.3. It was concluded from this study that the constant shear element gives better results than the ordinary element both for displacements and for stresses. However, one drawback of this new element is the fact that it yields a constant shear stress within each element. In general it is of great interest to know more in detail about the shear stress variation along the stiffeners. The shear stress obtained by this element is only representative of an average value at the centroid of the element.

For curiosity, the stress subroutine of the ordinary membrane element was combined in the computer program with the stiffness subroutine of the constant shear element. This combination gave the same stresses in x and y directions as the constant shear-stress routine, while an improved representation of the varying shear stress was obtained.

Both the ordinary membrane element and the constant shear element are made available in the computer program. The names of the stiffness and the stress subroutines are QUPSSP and PLSTSP respectively.

(*) It should be noted that the stiffness of this element is dependent on the element orientation relative to the global axes. This element should be modified for general quadrilateral configuration, see (22).

2.3 Plate Bending Element

The bending element used for the plate is a general compatible quadrilateral assembled from 4 triangular subelements as shown in Fig. 2.3. This type of element gives continuous slope and displacements between adjacent element boundaries. Each triangle is a so-called LCCT11 element or "linear curvature compatible triangle with 11 degrees of freedom". The seven internal degrees of freedom of the quadrilateral (see Fig. 2.3) are eliminated by static condensation. The individual bending triangles shown in Fig. 2.4 have been developed by Clough and Tocher, and are discussed more in detail in [6], [9] and [7].

The name of the bending stiffness subroutine in the program is Q19. This subroutine assembles 4 triangular subelements by calling the triangular element plate bending stiffness routine SLCT11. The corresponding bending moment routines are BMQ19 and BMQ12.

2.4 Membrane Element for the Stiffeners.

Fig. 2.5 shows the element types used for idealizing the stiffeners. The elements used are spar elements that are specially designed to represent the axial, bending and shear action of web type structures. The polynomial expansions of the u and v displacements are different along the two element axes. In matrix form these displacements are given by

$$u = < \phi_u > \{v_i\}$$

$$v = < \phi_v > \{v_i\}$$

where, for the element in Fig. 2.5b, the nodal point displacement vector and the interpolation polynomials are given by

$$\{v_i\}=\begin{Bmatrix} u_1 \\ u_3 \\ u_5 \\ u_6 \\ u_7 \\ u_8 \\ \hline v_2 \\ v_4 \\ \hline \theta_9 \\ \theta_{10} \end{Bmatrix} \quad <\phi_u>^T = 1/4 \begin{bmatrix} (1-\xi)(1-\eta) \\ (1+\xi)(1-\eta) \\ (1+\xi)(1+\eta) \\ (1-\xi)(1+\eta) \\ (1-\xi^2)(1-\eta) \\ (1-\xi^3)(1+\eta) \\ \hline 0 \\ 0 \\ \hline 0 \\ 0 \end{bmatrix} \quad <\phi_v>^T = 1/4 \begin{bmatrix} 0 \\ 0 \\ 0 \\ 0 \\ 0 \\ 0 \\ \hline 2-3\xi+\xi^3 \\ 2+3\xi-\xi^3 \\ \hline 1-\xi-\xi^2+\xi^3 \\ -1-\xi+\xi^2+\xi^3 \end{bmatrix}$$

As for the membrane element of the plate, the sidenode displacements u_7 and u_8 are defined as deviations from the linear interpolation between the u displacements at the adjacent corner nodes. The element in Fig. 2.5a is similar to this refined element but does not have the midside nodes.

The rotations θ_9 and θ_{10} are eliminated by static condensation; this condensation is permissible because when the shear force is discontinuous, the angles θ will not be continuous between two adjacent elements. The static condensation operation results in a constant shear stress over the entire element. As seen from the interpolation functions, the displacement v does not vary through the height of the element. This constant implies that the strain ϵ_y is zero, and thus σ_y will not be zero (due to Poisson ratio effects). The stiffness subroutines, however, are adjusted so that the energy corresponding to σ_y is equal to zero.

The element stiffness subroutines for the spar elements are called SPAR6 and SPARC, the latter being the element that includes the two side nodes. Corresponding stress routines are FSPAR6 and FSPARC. It is seen that the midside node can match a midside node of the QUPSSP element. Based on the improved re-results obtained when retaining the midside nodes, use of the SPARC element is recommended. For this element it is also possible to condense one or two of the sidenodes.

Some other types of spar elements have been described by Argyris, et. al. [1] and by Sanders, et. al. [15]. A more recent study has been made by Willams [22]. From a review of this literature, it has been concluded that the elements incorporated into this program are the most efficient ones presently available.

2.5 Bar Element for Top Flanges.

Fig. 2.6 shows the bar element used to provide the top flange of the stiffeners. The axial displacement is given by

$$u = < \phi_u > \{u_i\}$$

where

$$\{u_i\} = \begin{Bmatrix} u_1 \\ u_2 \\ u_3 \end{Bmatrix} \qquad < \phi_u >^T = \begin{Bmatrix} 1/2\ (1 - \xi) \\ 1/2\ (1 + \xi) \\ (1 - \xi^2) \end{Bmatrix}$$

As for the other elements, the midside displacement u_3 is defined as deviation from the linear interpolation between u_1 and u_2. The axial stress varies linearly along the element. However, if the midside node is not included, the stress will be constant.

The stiffness matrix for this element is given by

$$[K] = \frac{AE}{L}\begin{bmatrix} 1 & -1 & 0 \\ -1 & 1 & 0 \\ 0 & 0 & \frac{16}{3} \end{bmatrix}$$

The name of the stiffness subroutine is BAR while the corresponding routine calculating the axial stress is BARST.

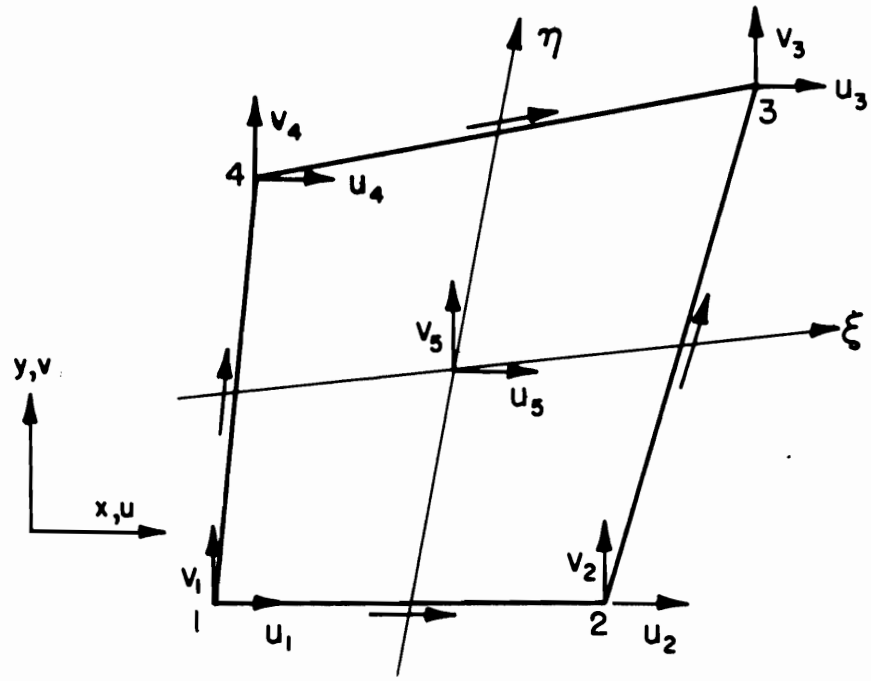

FIG. 2.1 MEMBRANE ELEMENT FOR THE PLATE

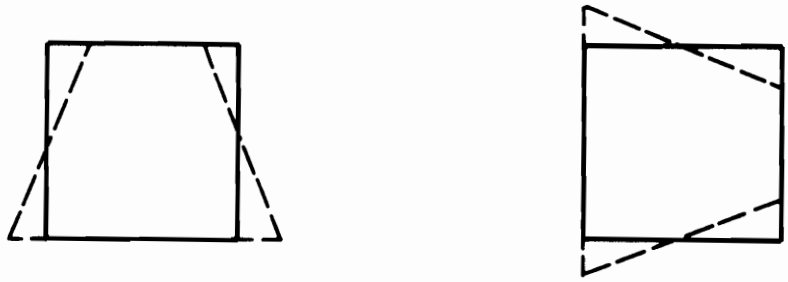

FIG. 2.2 TYPICAL BENDING MODES OF THE MEMBRANE ELEMENT

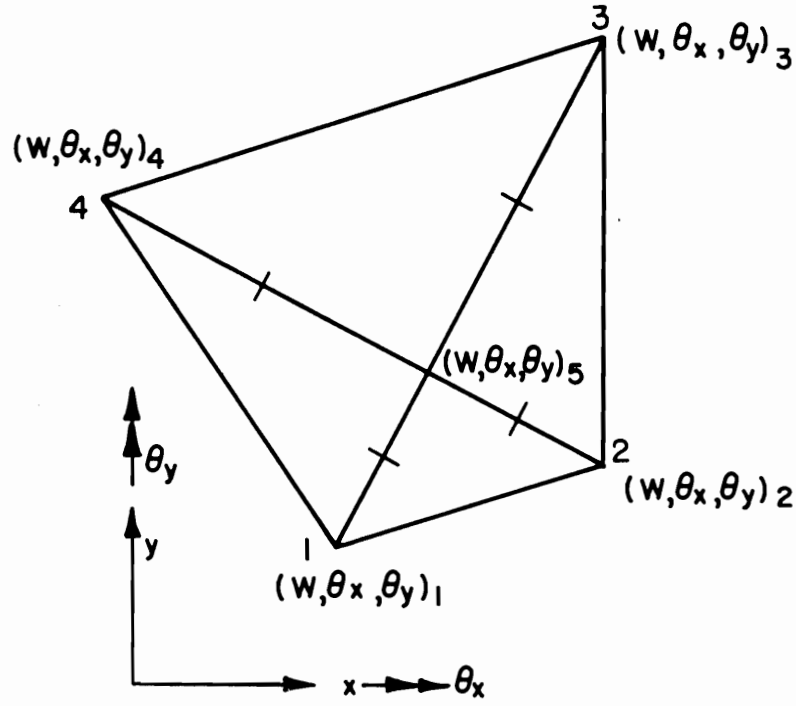

FIG. 2.3 PLATE BENDING QUADRILATERAL

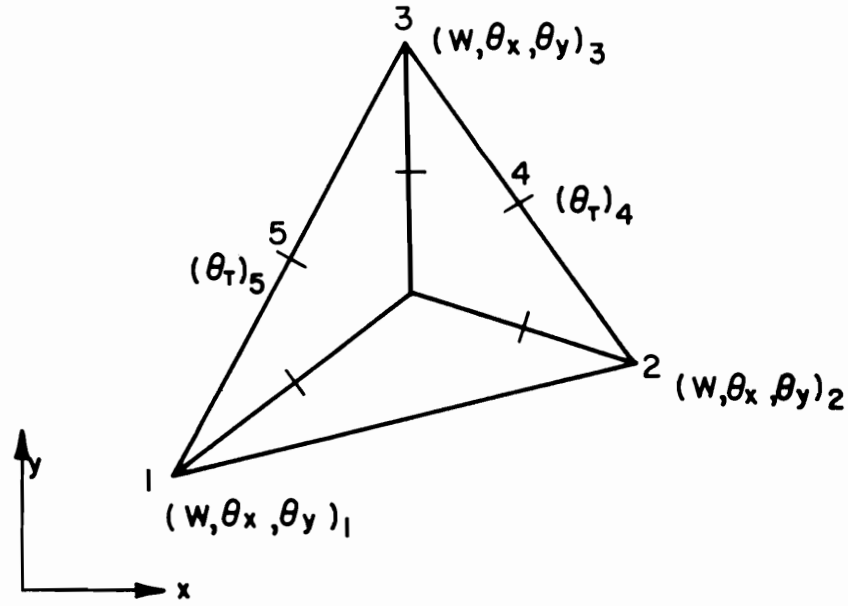

FIG. 2.4 LCCT11 PLATE BENDING TRIANGLE

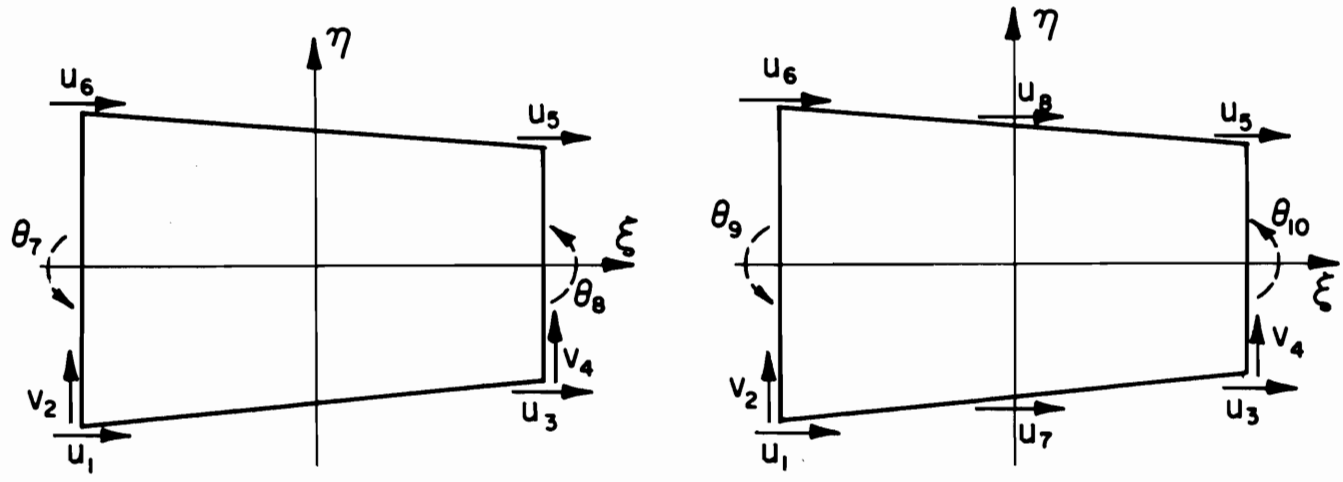

a) BASIC ELEMENT

b) REFINED ELEMENT

FIG. 2.5 "SPAR" ELEMENTS FOR THE STIFFENERS

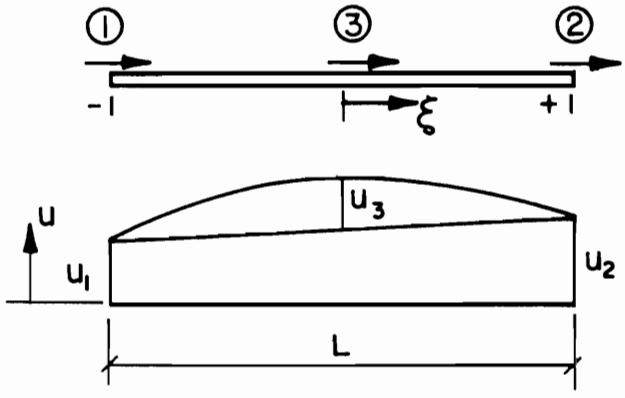

FIG. 2.6 BAR ELEMENT

3. COMPUTER PROGRAM "LASP"

3.1 Structure of the Program.

Figure 3.1 shows a flow chart of subroutines for the computer program LASP ("Linear Analysis of Stiffened Plates"). A short description of the different subroutines will be given in the following. However, the stiffness and the stress subroutines have been discussed in the preceding chapter, and their functions will not be repeated here.

MAIN is the main program. It reads some control quantities and calls the mesh generator or the input routine called INFORM.

MESH generates a finite element mesh and corresponding information needed by the program for the analysis of a rectangular plate with orthogonal stiffening. A more detailed description will be given in Section 3.2.

INFORM reads and prints input data when the mesh generator is not used, also see Section 3.3.

STIFF calculates the bandwidth of the system stiffness matrix. Then it calls the different stiffness subroutines and assembles the system stiffness matrix. The element stiffness routines are only called for elements of different geometry, so that if all elements are alike, only one call is made. STIFF also introduces the boundary conditions into the total stiffness matrix.

BANSOL solves the total system of equations using Guassian elimination. Only half the band of the symmetric stiffness matrix is used. BANSOL operates in core only.

STRESS calls the element stress subroutines for computation of membrane and plate bending stresses. The nodal point values are found by taking the

arithmetic average of the corresponding corner values of all elements adjacent to that nodal point. The principal surface stresses and their directions are calculated at all nodal points of the plate.

QLOAD calculates nodal point loads for a general quadrilateral subjected to transverse load. A simplified displacement polynomial is used in this load subroutine so that the distributed load is converted into concentrated nodal loads only (moment forces corresponding to θ_x and θ_y are not included). This simplification has negligible influence on the results.

3.2 Use of Mesh Generator.

The mesh generator can be used for rectangular plates with orthogonal stiffening when the plate has constant thickness and the stiffeners are continuous and have constant cross-section. The boundary conditions and the loading may be arbitrary. The data generation is made as extensive as possible to minimize the necessary input information. Furthermore, the mesh generator does not require that the program user have any knowledge about the finite element method. However, as for any finite element program, some understanding of the finite element method is an advantage when interpreting the computed results.

For each data set to be generated, the following data cards are needed (compare data sheet for the following example).

A. < START 1 > (6H)

This word that starts in column 1 on a separate card initiates the use of the mesh generator.

B. < HEADLINE . . . . > (78 H)

Headline for the output.

C. < ML, NL, NSX, NSY, ICCODE, LCODE, NLOAD > (715)

ML = number of coordinate points on the x-axis (see example)

NL = number of coordinate points on the y-axis

NSX = number of stiffeners in x-direction

NSY = number of stiffeners in y-direction

ICCODE = number of boundary condition cards (see also G.). $1 \leq$ ICCODE ≤ 8

LCODE = code for distributed transversal load. LCODE can have the following values:

0, no distributed transversal load.

-1, uniformly distributed load.

>0, LCODE number of elements have distributed load.

NLOAD = number of nodal point that have concentrated loads. These loads will be added to the distributed load.

D. < Thickness, E, ν > (3F10.3)

This card gives plate thickness, Young's modulus and Poisson's ratio.

E. < XX (J), J = 1, ML > (8F10.5)

< YY (J), J = J, NL > (8F10.5)

The vector XX contains, in increasing order, the location of the coordinate points on the x-axis and YY the points on the y-axis. Both the information for XX and for YY must begin on a new card. It is not necessary that every

coordinate value be given. When some values are omitted, these values are generated by linear interpolation between the values at the closest points where values are given. No extrapolation is performed, consequently the values XX(ML) and YY(NL) must always be given.

F. < J, HX (J), TX(J), AX(J) > (I5, 3F10.5)

< J, HY (J), TY(J), AY(J) > (I5, 3F10.5)

One card is required for every stiffener in x-direction and one card for every stiffener in y-direction.

On the card for a stiffener in x-direction

J is coordinate point number,

HX(J) is height of stiffener in x-direction,

TX(J) is thickness of stiffener in x-direction,

AX(J) is flange area of stiffener in x-direction,

H(Y) etc., is defined similarly.

G. < J, U, V, W, θ_x, θ_y, U_T, V_T > (8I2)

The displacement boundary conditions are given on ICCODE number of cards. Each card must contain the following information:

J is a code telling where the following boundary conditions apply. J can have values from 1 to 8. When J is less than 5, it refers to the side number, see figure 3.2. When greater than 4, J refers to a corner where special boundary conditions are imposed. The boundary conditions for the sides are also valid for the adjacent corner points. When two sides that have different boundary conditions meet at a corner, "maximum fixity" is

assumed for the corner. This means that all the displacement components that are fixed for either one of the adjacent sides will be assumed to be fixed at the corner.

< U, V, W, θ_x, θ_y > = boundary conditions for the plate. The following codes are allowed.

0 = free component

1 = fixed component

< U_T, V_T > = boundary condition for the axial displacement at the top of the stiffeners at that side (or corner)

0 = free component

1 = fixed component

H. < node number, F_x, F_y, F_z, T_x, T_y > (I5, 5F10.5)

The concentrated loads are given on NLOAD number of cards. F_x, F_y and F_z are the load components in the x, y and z directions respectively. T_x and T_y are torques along the x and the y axes.

If the nodal point is located at the top of a stiffener and has one degree of freedom in y-direction, the corresponding force component must be punched in columns 6 to 15.

If NLOAD is equal to zero, these cards must be omitted.

I. Distributed transverse load. When LCODE is equal to -1, the transverse load is assumed to be uniformly distributed and its intensity q is given by one card only:

< q > (F10.5)

When LCODE is greater than zero, LCODE elements have transversal (not necessarily uniform) load:

< J, q_1, q_2, q_3, q_4 > (15, 4F10.5)

Here J is the element number and q_1, q_2, q_3 and q_4 are corner intensities of the transversal load expressed in units of force per unit area.

J. < STOP > or < START1 > or < START2 > (6H)

The word STOP will terminate the computation process while START1 or START2 indicates another data set. The use of the word START2 will be explained in the next section.

EXAMPLE

The use of the mesh generator will now be illustrated by an example. Fig. 3.3 shows a plate with three stiffeners. The plate is fixed at one side, simply supported at another side, and has two free edges. The global coordinate system has its origin at the lower left corner. The plate is divided into 24 elements such that there are 4 elements along the x-axis and 6 elements along the y-axis. Hence there are 5 coordinate points on the x-axis and 7 on the y-axis. The two stiffeners in the x-direction pass through at coordinate points 4 and 7 at the y-axis. The stiffener in the y-direction passes through coordinate point 5 at the x-axis. The input sheet for this case is shown in figure 3.4.

It is important to note that the global system axes should always be oriented so that there are fewer elements along the x-axis than along the y-axis so that the band width of the system matrix will be minimized. Thus in this example the x axis has been taken in the 4 element wide direction while the y axis is in the 6 element wide direction.

When concentrated forces act at a nodal point, one must know how the automatic nodal point numbering is carried out. The numbering always starts at the origin and goes by rows in the x-direction. Where there are stiffeners there are always two nodal points at each mesh grid point (one at the top of the stiffener, see Fig. 3.6). In addition, there is one lower midside node for each spar-element, and one top midside node if the stiffener has a flange.

The element numbering goes like this: first come all plate elements, then all spar-elements and last all BAR-elements. The plate element numbering starts in the lower left corner and goes by rows in x-direction. One can always easily find out from the output how the elements and nodes are numbered. A figure

showing the node numbering is printed, as in Fig. 3.6, and for each element the connected nodal points are listed.

3.3 Input when the Mesh Generator is not used

When the mesh generator is not used, the program can be applied to more general stiffened plate problems. The plate can have arbitrary shape, but the stiffening must still be orthogonal. The program allows cut-outs and discontinuous stiffeners.

The input information is much more extensive than when the mesh generator is used. The data cards required are as follows:

A. < START2> (6H)

This word that starts in column 1 tells that the mesh generator is not going to be used.

B. < HEADLINE . . . .> (78H)

Headline for the output.

C. < NUMEL, NUMNP, NUMBC, NMAT, NDIFFE, NLOAD, LCODE, RT > (7I5, F10.5)

The different symbols stand for

NUMEL = total number of elements

NUMNP = total number of nodal points

NUMBC = number of points where boundary conditions are imposed

NMAT = number of different material laws

NDIFFE number of different elements, i.e., number of different element

stiffness matrices (considering both membrane and plate bending stiffness). For instance, if all elements are alike, NDIFFE = 1

NLOAD = number of nodal points that have concentrated loads

LCODE = code for distributed load, see section 3.2

RT = reference thickness

D. < I, ICODE, E, ν > (I3, I2, 2E10.3)

where

I = material number (less than or equal to NMAT)

ICODE = can have two values

0 = isotropic material

1 = general orthotropic material

However, the present version of the program permits only an isotropic material.

E = Youngs modulus

ν = Poisson's ration

One data card is reuqired for each material.

E. < N, (EGEOM (N,I), I = 1, 8), THICK(N), MAT(N) > (I3, 9F8.4, I3)

Here, the geometry for each element of different type is given.

N = element stiffness number (the stiffness matrices of different type have to be numbered)

< EGEOM (N,I), I = 1, 8 > are the local corner point coordinates X1, X2, X3, X4, Y1, Y2, Y3, Y4

Local corner numbering is counter-clockwise and starts in the lower left

corner. For bar elements, the length of the element is given by X2-X1.

THICK(N) = thickness of the element. If no value is given (=0), the reference thickness RT is assumed for that element. For bar elements, THICK(N) stands for the area of the flange.

MAT(N) = material law number (see under D). If not specified, material 1 is assumed.

One card is needed for each stiffness matrix of different type.

F. < N, IETYPE(N), (NP(N,I), I = 1, N1) > (815)

where

N = element number

IETYPE(N) = stiffness matrix number (corresponds to data in E.)

(NP(N,I), I = 1, N1) is the global nodal point numbering. N1 is number of each nodal points for that element (N1 ≤ 6)

The numbering starts in lower left corner and goes around counter-clockwise, Midside nodes follow after corner nodes.

Examples:

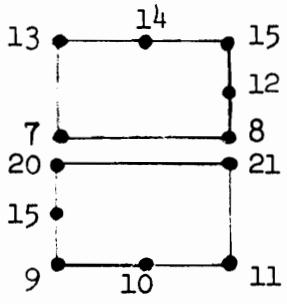

(7, 8, 15, 13, 12, 14)

(9, 11, 21, 20, 15, 10)

One card must be used for each element.

G. < N, I1, I2, I3 > (I5, 3I2)

These numbers specify the type of element stiffnesses that should be used. This information is given for all stiffness matrices of different type.

N = stiffness number (corresponds to N in E).

I1= indicates the membrane stiffness routine that should be used.

I1 can have the following values:

I1 = 3, use QUPSSP

I1 = 4 use SPAR6

I1 = 5 use SPARC

I1 = 6 use BAR with 2 nodes

I1 = 7 use Bar with 3 nodes

I2 indicates the plate bending stiffness that should be used

I2 can have only the value I2 = 1 that gives the Q19 plate bending quadrilateral. I2 = 0 for stiffener and flange elements.

I3 is an additional code that is needed to locate the additional nodes for the membrane elements. When the element is a QUPSSP, I3 can have the following values:

I3 = 0 no additional sidenode.

I3 = 1, 2, 3, or 4, for sidenode on side 1, 2, 3, or 4 respectively. Side 1 is the lower side and then the numbering goes counter-clockwise.

I3 = 5, 6, 7, or 8 when the quadrilateral has two sidenodes. For each case the the location of sidenodes are given in the figure below.

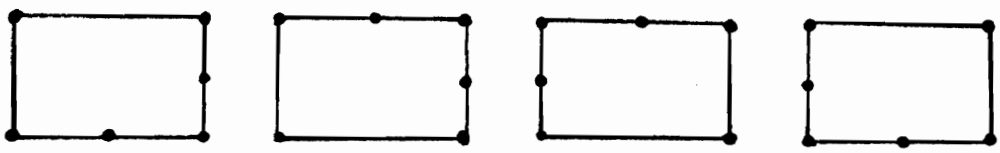

I3 = 5 I3 = 6 I3 = 7 I3 = 8

Other combinations of sidenodes are not allowed; they are not necessary either since there always should be at least two elements between two parallel stiffeners.

For the SPAR6 element I3 has the following meanings:

I3 = 1 The stiffener element is oriented parallel to the x-axis.

I3 = 2 The stiffener element is oriented parallel to the y-axis.

For the SPARC element I3 can have the following values:

I3 = 1, 2,

or 3 the SPARC-element is oriented in the x-direction.

I3 = 4, 5,

or 6 the SPARC-element is oriented in the y-direction.

here again:

I3 = 1 or 4, the top midnode and the bottom midnode should be condensed. Do not use these values, use the SPAR6-element instead.

I3 = 2 or 5, the top midnode is condensed while the lower midnode is retained.

I3 = 3 or 6, both midnodes are retained.

For the BAR-element I3 can have the following values:

I3 = 0, the element is oriented in x-direction.

I3 = 1, the element is oriented in y-direction.

H. <NDIM (I), I = 1, NUMNP> (40I2)

Give number of degrees of freedom at each nodal point. This information should start on a new card and must continue over as many cards as necessary.

I. <NBC (I), (NTAG (I,J), J = 1, N)> (I5, 512)

This information gives the boundary conditions. NBC (I) is the number of the nodal point where the boundary conditions are imposed. The boundary conditions are stored in the matrix NTAG. N is the number of degrees of freedom at the nodal point. The code that is used for NTAG can have the following values:

0 = free component

1 = fixed component

The ordering of the displacement components is u, v, w, θ_x, θ_y. Note that if some of the components are missing at a node, the boundary conditions should be condensed. For example, if at node 9 the only displacement component v is fixed, the boundary condition is then given by

< bbbb9b1bb .... > (b = blank)

One card is needed for each boundary condition point, NUMBC cards in total.

J. < J, (RDUM (I), I = 1, N)> (I5, 5F 12.5)

This information gives the concentrated nodal loads when NLOAD is greater than zero. J is the number of the nodal point and (RDUM (I), I = 1, N) are the load components. The ordering of the load components is F_x, F_y, F_z, T_x, T_y. If the nodal point has less than 5 components, the actual components are condensed to the left (as in I). A separate card must be used for every nodal point having concentrated loads.

K. Distributed transverse load.

When LCODE on card C is equal to -1, the load is uniformly distributed over the entire plate and the transverse load is given by one value only:

< q > (F12.5)

When LCODE is greater than zero, LCODE number of elements have distributed transversal load. This load is then given element-wise like:

< J, q_1, q_2, q_3, q_4 > (I5, 4F12.5)

where J is the element number and q_1, q_2, q_3 and q_4 are the corner intensities of the distributed load.

L. <STOP> or <START1> or <START2> (6H)

STOP is used in the case when there is no more data and START1 or START2 is used in the case of new data sets. This information must start in column 1.

EXAMPLE

A cantilever beam with a concentrated end load as shown in Fig. 3.5 is used as an example of input when the mesh generator is not used. The mesh generator could also have been used for this case, making the input much simpler. The direct data input is presented here merely as an example of the procedure. The figure shows a listing of the data cards and the finite element idealization of the beam.

3.4 Computer Output

The first part of the computer output is a full print of the input information. When the mesh generator is used, a figure of the generated mesh including stiffeners is printed out. This figure is very useful when interpreting the results. Fig. 3.6 shows this figure for the example in section 3.2. The mesh generator also prints out generated data, that is, data that would have had to be given as input if the mesh generator had not been used.

After that follows a table of the computed displacements at all the nodal points. The nodal point stresses for all the elements are then printed out. The stresses and the moments are averaged at the nodal points and their principal calues are calculated and printed out in two separate tables. Finally, the surface stresses and their principal values with corresponding angles are given. As an example, some important parts of the output for the cantilever beam are shown on pages 34 to 38.

3.5 Capacity of the Program

LASP operates only in core, consequently, its capacity is limited. However, the program could easily be extended to use external storage, resulting in a much larger capacity of the program.

Before summarizing the capacity of the different parts of the program, it should be repeated that the program calculates the stiffness matrix for identical elements only once. When a structure is divided into many identical elements, a substantial amount of computer time and storage is saved in this manner.

Upper limits of some of the variables in the program are:

NUMEL ≤ 100 (total number of elements)

NUMNP ≤ 150 (total number of nodal points)

NUMBC ≤ 50 (total number of points where boundary conditions are imposed)

NDIFFE ≤ 50 (number of different elements)

All these restrictions may be changed easily by updating the labeled common block called /IS/. Other limitations in this common block that may be changed easily are:

a) Total number of displacement components ≤700. (Dimensions of system stiffness matrix.)

b) Number of different material laws ≤5.

Another limitation is the capacity of matrix B in the labeled common block called /STORE/. Matrix B is used for storing the part of the stiffness matrixes that is needed for recovering the condensed internal degrees of freedom when calculating the stresses. The capacity of B is 1500.

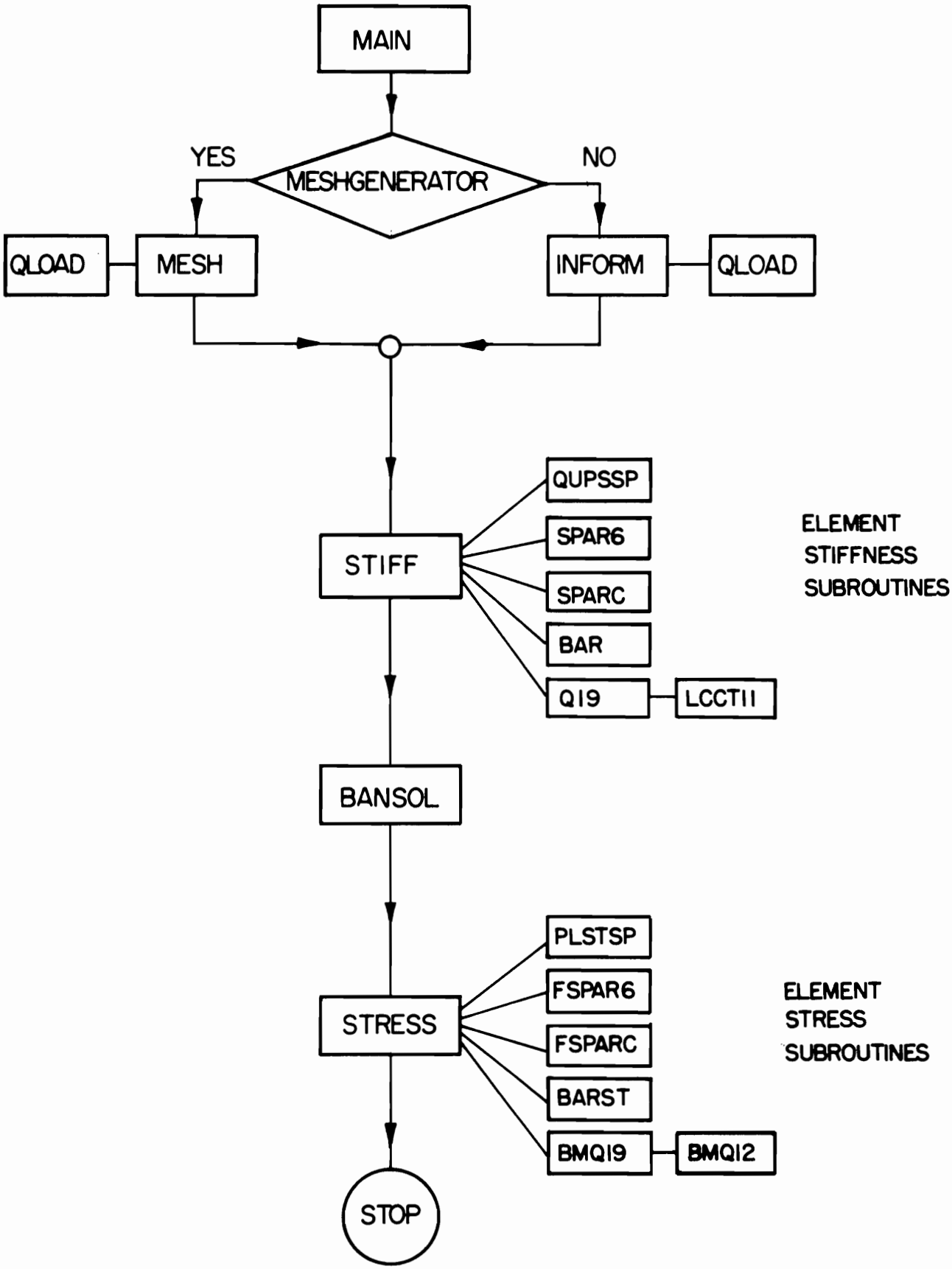

FIG. 3.1 FLOWCHART OF SUBROUTINES

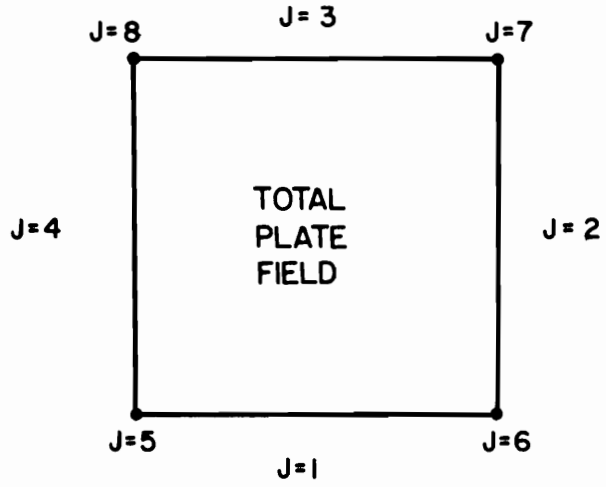

FIG. 3.2 EXPLANATION OF CODE J FOR THE BOUNDARY CONDITIONS

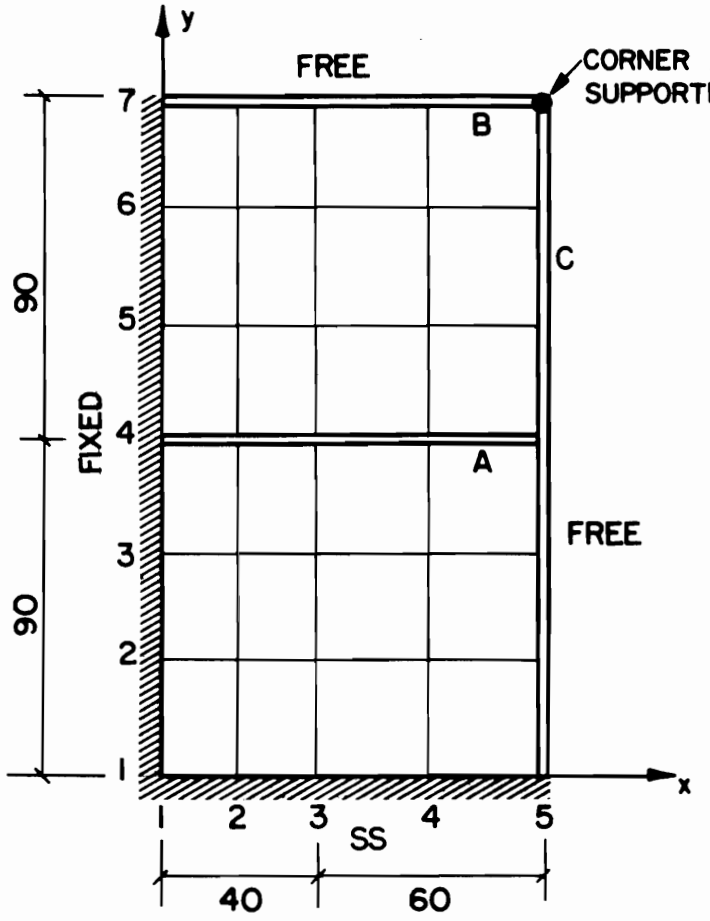

Plate thickness 0.7
Young's mod. 3.10^7
Poisson's ratio 0.3

Stiffeners:

	Height	Thickness	Flange Area
A	20	0.5	8
B	30	0.5	10
C	40	0.8	12

Uniform pressure 10 psi

FIG. 3.3 EXAMPLE OF USE OF THE MESH GENERATOR

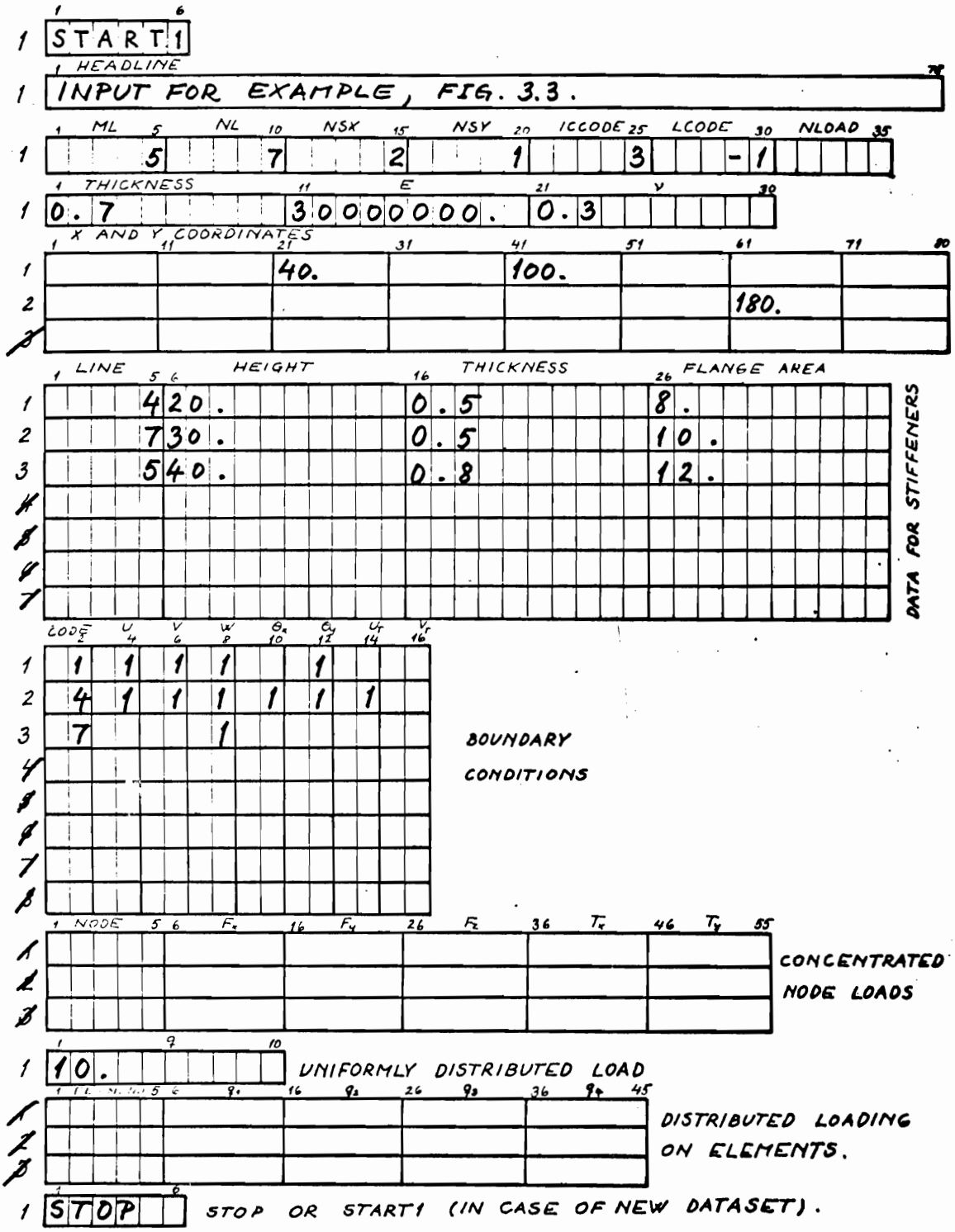

FIG. 3.4 INPUT DATA FOR MESHGENERATOR

```
START2
CALCULATION OF CANTILEVER BEAM WITH LONGITUDINAL AXIS IN Y DIRECTION
   15    29     9     1     3     1     0    0.02
  1 0     2.0E+5  0.3
  1          0.5       0.5                                    2.0       2.0
  2          0.5       0.5                                    2.0       2.0
  3          2.0       2.0                                    1.0       1.0       .01
    1     1     2     1     6     7
    2     2     3     2     7     8     5
    3     3     3     8     9     4     5
    4     1     7     6    11    12
    5     2     8     7    12    13    10
    6     3     8    13    14     9    10
    7     1    12    11    16    17
    8     2    13    12    17    18    15
    9     3    13    18    19    14    15
   10     1    17    16    21    22
   11     2    18    17    22    23    20
   12     3    18    23    24    19    20
   13     1    22    21    26    27
   14     2    23    22    27    28    25
   15     3    23    28    29    24    25
    1  3  1
    2  3  1  4
    3  5     5
  5  5  5  1  1  5  5  5  1  1  5  5  5  1  1  5  5  5  1  1  5  5  5  1  1  5  5  5  1
    1  1  1  1  1  1
    2  1  1  1  1  1
    3  1  1  1  1  1
    4  1
    8  1           1
   13  1           1
   18  1           1
   23  1           1
   28  1           1
   28                              1.5
STOP
```

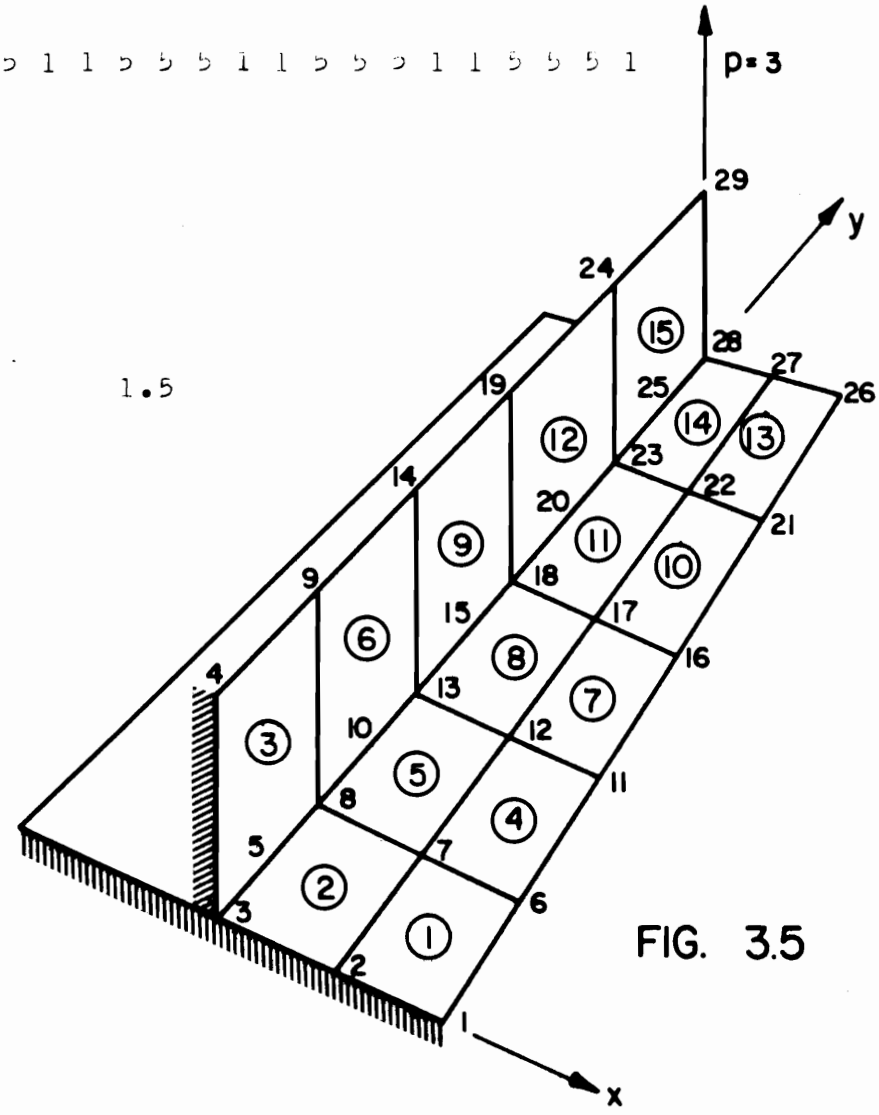

BEAM THEORY
δ = 1.0215

CALCULATED
δ = 1.020

FIG. 3.5

PICTURE OF NODAL POINT NUMBERING OF PLATE WITH STIFFENERS

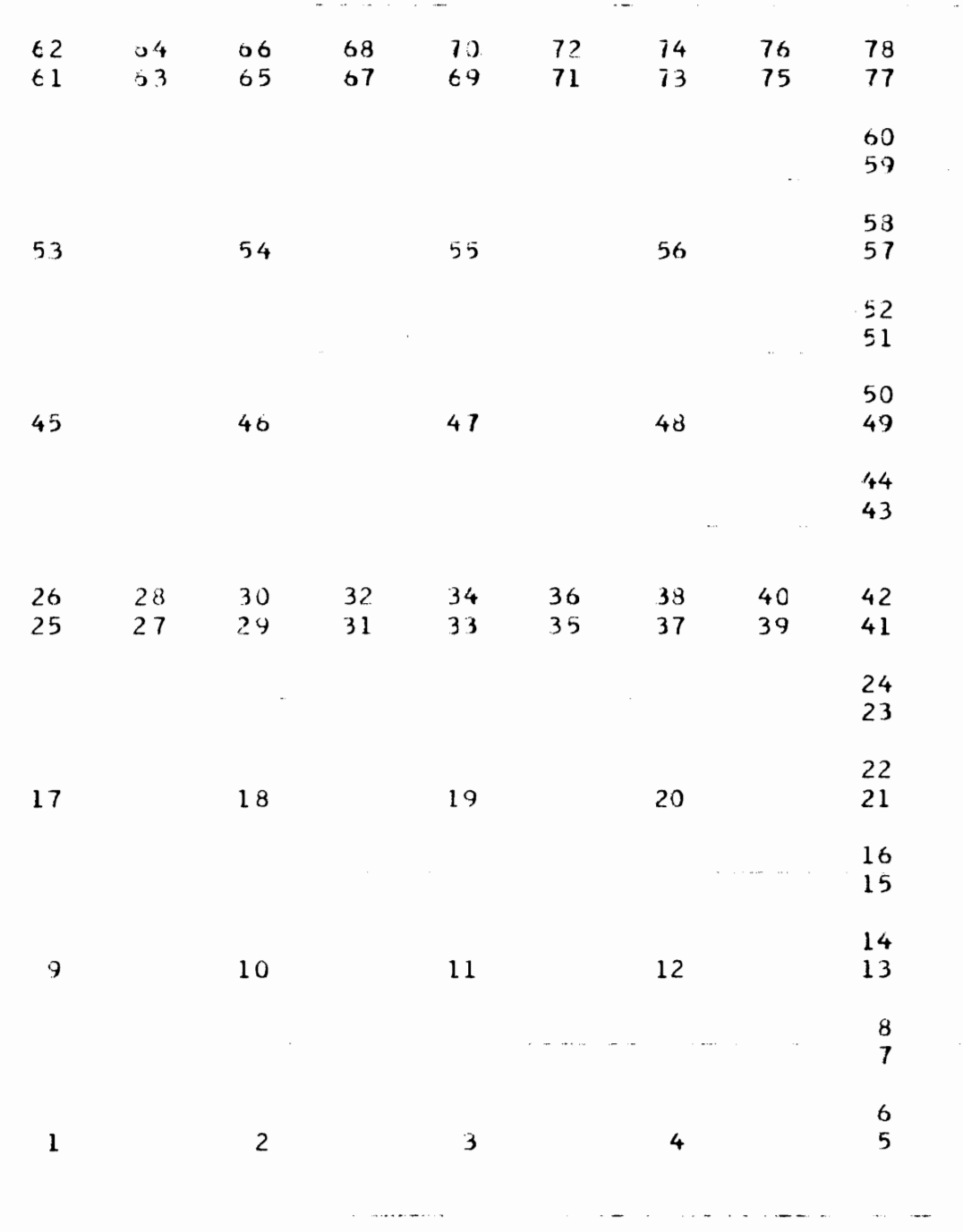

FIG. 3.6 ELEMENT MESH AND NODAL POINT NUMBERING GENERATED BY THE COMPUTER

TOTAL DISPLACEMENT VECTOR

NODE NO.	DISPL. 1	DISPL. 2	DISPL. 3	DISPL. 4	DISPL. 5
1	0.	0.	0.	0.	0.
2	0.	0.	0.	0.	0.
3	0.	0.	0.	0.	0.
4	0.				
5	.4230438E-03				
6	-.1540208E-02	.8627258E-02	.5677085E-01	.5606410E-01	.7259716E-02
7	-.7677851E-03	.8595708E-02	.5923429E-01	.5616740E-01	.3192881E-02
8	0.	.8847960E-02	.6000337E-01	.5622397E-01	0.
9	-.4491212E-01				
10	.5199622E-03				
11	-.8446290E-03	.1539333E-01	.2134029E+00	.9834214E-01	.5293863E-02
12	-.4317780E-03	.1582891E-01	.2153934E+00	.9808674E-01	.2713811E-02
13	0.	.1591784E-01	.2160585E+00	.9802674E-01	0.
14	-.7993866E-01				
15	.4972220E-03				
16	-.5957538E-03	.2060273E-01	.4423710E+00	.1284635E+00	.3619494E-02
17	-.2876812E-03	.2067792E-01	.4437242E+00	.1281691E+00	.1796184E-02
18	0.	.2092853E-01	.4441745E+00	.1280774E+00	0.
19	-.1049380E+00				
20	.4704119E-03				
21	-.3241563E-03	.2345655E-01	.7192584E+00	.1462562E+00	.1831779E-02
22	-.1814797E-03	.2377243E-01	.7199746E+00	.1460250E+00	.9284497E-03
23	0.	.2391328E-01	.7202204E+00	.1459718E+00	0.
24	-.1199268E+00				
25	.5034695E-03				
26	.8318830E-04	.2451568E-01	.1019646E+01	.1522622E+00	.8889903E-03
27	.9970844E-04	.2469981E-01	.1020076E+01	.1521584E+00	.7038716E-03
28	0.	.2492306E-01	.1020320E+01	.1522734E+00	0.
29	-.1249305E+00				

AVERAGED MEMBRANE STRESSES AT NODAL POINTS

NODE NO.	NO. OF ELEM.	SIGMA-X	SIGMA-Y	TAU-XY	SIGMA-1	SIGMA-2	ANGLE(DEGR.)
1	1.	.2844151E+03	.9480503E+03	-.4195756E+02	.9506925E+03	.2817729E+03	3.6033
2	2.	.2833750E+03	.9445833E+03	-.5975788E+02	.9499406E+03	.2780177E+03	5.1229
3	1.	.3474770E+03	.1158257E+04	-.7755820E+02	.1165609E+04	.3401245E+03	5.4154
6	2.	-.8579031E+02	.7439296E+03	-.2659933E+02	.7447814E+03	-.8664216E+02	1.8343
7	4.	-.7759109E+02	.7681684E+03	-.5096720E+02	.7712287E+03	-.8065140E+02	3.4362
8	2.	-.6871580E+02	.7946608E+03	-.7533506E+02	.8011849E+03	-.7523996E+02	4.9496
11	2.	.1592501E+02	.6035513E+03	-.2148697E+02	.6043359E+03	.1514037E+02	2.0913
12	4.	.1352464E+02	.6081681E+03	-.4760743E+02	.6119555E+03	.9737289E+01	4.5485
13	2.	.7838424E+01	.6018321E+03	-.7372789E+02	.6108466E+03	-.1176050E+01	6.9708
16	2.	-.2506305E+01	.4024092E+03	-.2727473E+02	.4042381E+03	-.4335245E+01	3.8363
17	4.	.2201054E-02	.3971765E+03	-.5130263E+02	.4036962E+03	-.6517490E+01	7.2425
18	2.	.3572075E+01	.3954818E+03	-.7533054E+02	.4094626E+03	-.1040876E+02	10.5141
21	2.	.1784120E+01	.1961824E+03	-.2401879E+02	.1991061E+03	-.1139539E+01	6.9401
22	4.	-.4948358E+01	.1996097E+03	-.4964824E+02	.2110230E+03	-.1636167E+02	12.9464
23	2.	-.1174787E+02	.2028134E+03	-.7527769E+02	.2265895E+03	-.3552396E+02	17.5285
26	1.	.2765455E+02	.1142087E+03	-.2522093E+02	.1210215E+03	.2084170E+02	15.1163
27	2.	.4885590E+02	.1073941E+03	-.4972955E+02	.1358286E+03	.2042138E+02	29.7602
28	1.	.1072566E+02	-.9719237E+02	-.7423817E+02	.4854291E+02	-.1350096E+03	-26.9945

MIDPOINT MEMBRANE STRESSES

ELEM.NUMBER	SIGMA-X	SIGMA-Y	TAU-XY	SIGMA-1	SIGMA-2	ANGLE(DEGR.)
1	.1141317E+03	.8953878E+03	-.4195756E+02	.8976347E+03	.1118849E+03	3.0653
2	.1187890E+03	.9078201E+03	-.7755820E+02	.9153714E+03	.1112376E+03	5.5610
4	-.2974235E+02	.6910415E+03	-.1124111E+02	.6912167E+03	-.2991762E+02	.8933
5	-.2787512E+02	.7067917E+03	-.7311192E+02	.7139969E+03	-.3508034E+02	5.6284
7	.7353184E+01	.5051263E+03	-.3173282E+02	.5071411E+03	.5338386E+01	3.6330
8	.4399679E+01	.4943051E+03	-.7434386E+02	.5053384E+03	-.6633626E+01	8.4416
10	-.1016344E+01	.2971116E+03	-.2281665E+02	.2988477E+03	-.2752462E+01	4.3512
11	-.2904734E+01	.3030915E+03	-.7631722E+02	.3210692E+03	-.2088247E+02	13.2553
13	-.2243827E+01	.9865169E+02	-.2522093E+02	.1046049E+03	-.8197058E+01	13.2812
14	.1395934E+02	.1010453E+03	-.7423817E+02	.1435680E+03	-.2856333E+02	29.8035

AVERAGED STRESSES IN THE STIFFENERS

NODE NO.	NO. OF ELEM.	SIGMA-X	TAU-XZ	NO. OF ELEM.	SIGMA-Y	TAU-YZ
3				1.	.1054013E+04	.1499224E+03
4				1.	-.5025588E+04	.1499224E+03
8				2.	.8152755E+03	.1499423E+03
9				2.	-.4006684E+04	.1499423E+03
13				2.	.5994806E+03	.1499604E+03
14				2.	-.2999014E+04	.1499604E+03
18				2.	.3944102E+03	.1499590E+03
19				2.	-.1996727E+04	.1499590E+03
23				2.	.2063378E+03	.1499601E+03
24				2.	-.1002935E+04	.1499601E+03
28				1.	-.1004101E+03	.1499610E+03
29				1.	.5020503E+02	.1499610E+03

AVERAGED BENDING MOMENTS AT NODAL POINTS

NODE NO.	NO OF ELEM.	M-XX	M-YY	M-XY	M-1	M-2	ANGLE(DEGR.)
1	1.	.4355142E-03	.4081302E-02	-.2205862E-03	.4094600E-02	.4222163E-03	3.4499
2	2.	.1617667E-02	.4853276E-02	-.7788933E-04	.4855150E-02	.1615793E-02	1.3782
3	1.	.1644741E-02	.5006491E-02	.2746041E-04	.5006715E-02	.1644517E-02	-.4680
6	2.	-.6013523E-04	.3365907E-02	-.9019769E-04	.3368280E-02	-.6250823E-04	1.5070
7	4.	.7226109E-04	.3168588E-02	-.4376327E-04	.3169206E-02	.7164266E-04	.8096
8	2.	.8705321E-04	.3091047E-02	.5529143E-05	.3091057E-02	.8704303E-04	-.1055
11	2.	-.1922955E-05	.2408834E-02	.8294126E-04	.2411685E-02	-.4773151E-05	-1.9681
12	4.	.2031730E-04	.2423293E-02	.3258139E-04	.2423735E-02	.1987562E-04	-.7767
13	2.	.3581721E-04	.2425916E-02	.3154830E-06	.2425916E-02	.3581717E-04	-.0076
16	2.	-.6406239E-05	.1595020E-02	.8190424E-04	.1599198E-02	-.1058430E-04	-2.9202
17	4.	-.1971471E-05	.1595413E-02	.4305416E-04	.1596573E-02	-.3131064E-05	-1.5428
18	2.	-.3027537E-05	.1595823E-02	.1882824E-05	.1595825E-02	-.3029754E-05	-.0675
21	2.	.2161638E-04	.7736402E-03	.6581383E-04	.7793565E-03	.1590009E-04	-4.9640
22	4.	-.2093463E-04	.7800933E-03	.2756925E-04	.7810411E-03	-.2188237E-04	-1.9689
23	2.	-.4104560E-04	.7809401E-03	.9883189E-06	.7809413E-03	-.4104679E-04	-.0689
26	1.	.2317399E-04	.3976548E-04	.4057067E-04	.7287986E-04	-.9940392E-05	-39.2218
27	2.	-.9814748E-04	.8217586E-06	.2622100E-05	.8911801E-06	-.9821690E-04	-1.5166
28	1.	-.3479250E-03	-.5810369E-04	-.1423182E-04	-.5740650E-04	-.3486222E-03	2.8045

MIDPOINT BENDING MOMENTS

ELEM.NUMBER	M-XX	M-YY	M-XY	M-1	M-2	ANGLE(DEGR.)
1	.6374400E-03	.3932282E-02	-.4793694E-03	.4000609E-02	.5691130E-03	8.1120
2	.7672487E-03	.3976554E-02	-.1489697E-03	.3983454E-02	.7603486E-03	2.6520
4	-.4865698E-04	.2791982E-02	.6722566E-04	.2793572E-02	-.5024703E-04	-1.3549
5	.5457376E-04	.2807109E-02	.1935140E-04	.2807245E-02	.5443772E-04	-.4028
7	.1639857E-04	.2011712E-02	.7325322E-04	.2014397E-02	.1371287E-04	-2.0997
8	-.2407364E-08	.2004434E-02	.2761836E-04	.2004798E-02	-.3665291E-06	-.7721
10	-.7764913E-05	.1185957E-02	.7398160E-04	.1190524E-02	-.1233249E-04	-3.5329
11	-.6353015E-05	.1189772E-02	.2581808E-04	.1190329E-02	-.6910033E-05	-1.2359
13	-.2608018E-04	.3968209E-03	.2384600E-04	.3981613E-03	-.2742052E-04	-3.2171
14	-.1025205E-03	.3837410E-03	.1210487E-05	.3837441E-03	-.1025235E-03	-.1426

AVERAGED SURFACE STRESSES

	TOP SURFACE				BOTTOM SURFACE			
NODE NO.	SIGMA-1	SIGMA-2	TAU-MAX	ANGLE(DEGR.)	SIGMA-1	SIGMA-2	TAU-MAX	ANGLE(DEGR.)
1	.7050189E+03	.2564376E+03	.2242907E+03	3.6787	.1196367E+04	.3071071E+03	.4446301E+03	3.5653
2	.6597952E+03	.1799064E+03	.2399444E+03	6.6359	.1240606E+04	.3756088E+03	.4324986E+03	4.2837
3	.8679987E+03	.2386609E+03	.3146689E+03	7.2894	.1464306E+04	.4405017E+03	.5119020E+03	4.2640
6	.5426936E+03	-.8290059E+02	.3127971E+03	1.9420	.9468729E+03	-.9038727E+02	.5186301E+03	1.7693
7	.5815752E+03	-.8544981E+02	.3335120E+03	4.1671	.9610606E+03	-.7603234E+02	.5185465E+03	2.9661
8	.6174787E+03	-.8221976E+02	.3498492E+03	6.2454	.9854864E+03	-.6885544E+02	.5271709E+03	4.0898
11	.4605966E+03	.1446507E+02	.2230657E+03	3.4067	.7484534E+03	.1543756E+02	.3665079E+03	1.2910
12	.4681592E+03	.6916979E+01	.2306211E+03	6.2051	.7563760E+03	.1193345E+02	.3722213E+03	3.5225
13	.4680401E+03	-.6073526E+01	.2370568E+03	9.0626	.7546827E+03	.2691840E+01	.3759954E+03	5.6527
16	.3100273E+03	-.5441275E+01	.1577343E+03	5.8876	.4991063E+03	-.3886683E+01	.2514965E+03	2.5504
17	.3107980E+03	-.9225820E+01	.1600119E+03	9.8399	.4976696E+03	-.4884361E+01	.2512770E+03	5.5899
18	.3178532E+03	-.1436704E+02	.1661101E+03	13.5060	.5025653E+03	-.7943646E+01	.2552545E+03	8.5691
21	.1548318E+03	-.4580660E+01	.7970624E+02	10.2707	.2442709E+03	.1411036E+01	.1214299E+03	4.7568
22	.1681225E+03	-.1901073E+02	.9356661E+02	16.6252	.2552261E+03	-.1501531E+02	.1351207E+03	10.4027
23	.1851479E+03	-.3847597E+02	.1118119E+03	21.1799	.2696047E+03	-.3414542E+02	.1518750E+03	14.8436
26	.1199834E+03	.1810348E+02	.5093996E+02	16.4405	.1221703E+03	.2346935E+02	.4935046E+02	13.7495
27	.1374398E+03	.2464981E+02	.5639497E+02	31.1010	.1343382E+03	.1607228E+02	.5913296E+02	28.4815
28	.6543964E+02	-.1275446E+03	.9649213E+02	-24.7551	.3226523E+02	-.1430937E+03	.8767944E+02	-29.4595
ELEM. NUMBER (MIDPOINT VALUES)								
1	.6597491E+03	.7558713E+02	.2920810E+03	1.2947	.1136407E+04	.1472957E+03	.4945557E+03	4.1106
2	.6770193E+03	.6496163E+02	.3060288E+03	6.4787	.1153977E+04	.1572603E+03	.4983584E+03	4.9975
4	.5239461E+03	-.2724655E+02	.2755963E+03	1.5886	.8586187E+03	-.3272005E+02	.4456694E+03	.4633
5	.5478921E+03	-.4067646E+02	.2942843E+03	7.3094	.8809352E+03	-.3031767E+02	.4556264E+03	4.5430
7	.3878452E+03	.2947734E+01	.1924487E+03	5.4101	.6270370E+03	.7129169E+01	.3099539E+03	2.5300
8	.3890417E+03	-.1060290E+02	.1998223E+03	11.1719	.6231188E+03	-.4148121E+01	.3136334E+03	6.7036
10	.2291877E+03	-.3783977E+01	.1164859E+03	6.7658	.3691802E+03	-.2393423E+01	.1857868E+03	2.8384
11	.2552284E+03	-.2604679E+02	.1406376E+03	16.8095	.3887378E+03	-.1754595E+02	.2031419E+03	10.7980
13	.8330059E+02	-.9137171E+01	.4621888E+02	17.6073	.1267945E+03	-.8142165E+01	.6746832E+02	10.3236
14	.1288184E+03	-.3068699E+02	.7975272E+02	34.3558	.1601712E+03	-.2829333E+02	.9423228E+02	25.9554

TOTAL TIME IN SECONDS FOR DATA SET NO. 1 3.818

4. EXAMPLES OF APPLICATION OF THE PROGRAM

4.1 General Remarks

In a ship structure many parts can be idealized as plate-stiffener combinations with rectangular boundaries subjected to in-plane and lateral loads. The stiffeners are the main load carrying members in these substructures whereas the plating is mainly intended to transmit the lateral loads to the stiffeners. However, the plating also acts as a flange for the stiffeners and membrane stresses are induced in the plating due to the bending of the stiffeners.

Orthogonally stiffened plates have been mostly analyzed by two different methods in the past (*):

(1) Plate fields with few stiffeners have been dealt with as open grillages i.e. grid-works of beam elements without plating. An effective width of plating as flange for stiffeners has been assumed. A large number of different methods have been proposed for the analysis of grid-works by different investigators. Most of these methods can be found in [5] and [11].

(2) Plate fields with many stiffeners have been idealized as plates having different stiffness properties in two orthogonal directions (orthotropic plate theory). The main contribution to this method of analysis was made by Schade [16, 17]. The method has developed further since its first application and different ways for the evaluation of stiffness properties of the equivalent orthotropic plate and the solution of the resulting equations have been suggested by different investigators.

(*) Reference [11] includes a summary of previous studies on the orthogonally stiffened plates.

Both above methods have several disadvantages which can be summarized as follows:

It is not possible to have an insight into the behavior of the plate-stiffener interaction by either of these methods. The success in both methods partly depends on proper estimation of the effective width of the plating as flange for the stiffeners. This estimation generally is difficult to make and will be discussed later. In the first method the determination of effective loads distributed on the stiffeners represents a complicated problem. In both of these methods it is difficult to account for the torsional rigidities of the stiffeners.

For plate fields stiffened in one direction only, the effective flange width of plating for various load and boundary conditions was given by Schade in 1951 [18] who used a stress function in harmonic form to satisfy the equilibrium equations of the plating. For a general orthogonally stiffened plate, various methods have been used to estimate this effective width value. For design purposes, the values which apply for the case of one-dimensional bending have been adapted. For plate fields under uniform load, it has been suggested [16, 17] that the spacing between parallel stiffeners be taken as the effective flange width, with the plate thickness increased by $\frac{1}{1-\nu^2}$ (ν being Poisson's ratio) to account for the biaxial state of stress in the plate field. Clarkson, based on experiments [5] has suggested different values of effective flange width to be used in different stages associated with the open-grillage method. Obviously no solution based on these values can be exact and completely reliable. Further investigations are required in order to obtain a better knowledge of the local behavior of the plating between stiffeners. More generally, due to the increasing importance of orthogonally stiffened plates

in the design of ship structures, it will be necessary to develop more refined methods for analysis of these substructures.

4.2 Analysis Using the Finite-Element Method

It is evident that application of the finite element method to the analysis of orthogonally stiffened plates avoids the main difficulties which, as mentioned in 4.1 are inherent in the two other methods. In fact, the complete plate-stiffener combination can be idealized as an assemblage of finite elements of different types, and application of the finite element method will demonstrate the complete behavior of the system under combined in-plane and lateral loads.

However, in structures having a large number of stiffeners, the finite element analysis will require a long computer time and a large capacity of the program, and such an approach may not be economical for general cases. To avoid these difficulties, in the case of linear systems, it is preferable to investigate two aspects of the problem separately.

(1) Local bending of the plate-stiffener system.

(2) Overall bending of the structural assemblage.

Each of these topics is discussed in the following paragraphs.

(1) Local bending

This aspect of the behavior is associated with local bending of plate panels surrounded by edge beams and includes the local sagging of beams between stiffener intersections. Boundary conditions for this problem are shown in Fig. 4.1. The beam intersections are assumed to be fixed and all other boundary conditions result from uniformity of the structure and the loading (*). This problem is particularly important in the case where one set of stiffeners is significantly different from the other set [5]; it can be

(*) Note that one-half of each beam at one side of its plane of symmetry should be included in the analysis.

conveniently handled by the present program. In fact, as will be seen later, it has been studied in detail in this investigation and the effects of different parameters on the stress distribution have been demonstrated.

(2) Overall Bending

This part of the problem involves the computation of deflections and stresses of the whole plate field under concentrated loads acting at stiffener-intersections. These loads are mainly the reverse of the reactions at the supports as obtained in local bending analysis; in case of non-uniformity of the field or the loading these loads will include moments as well as forces.

Based on the linearity of the structure, the solution of the entire problem can be obtained by combining the solutions of these two parts.

In principle, the present finite element program can solve both parts of the complete problem in one step. However, because of capacity limitations it usually will be applied to solution of the local bending problem of a plate with many stiffeners.

As mentioned previously, the present finite element program is intended to be used to solve problems associated with bending and stretching of plate fields stiffened in one or two directions. The stiffeners are assumed to be on one side only of the plate surface, i.e., they are eccentric to the mid-surface. The stiffened plate can be subjected to combined in-plane and lateral loads. However, any problem handled by the program is subject to following restrictions:

1. Material is linearly elastic and isotropic.
2. Deflections are small so that the linear theory of deformations can be applied.

In general, a large number of such problems are encountered in the design of ship structures. It is, of course, not the purpose of this chapter

to investigate all possible combinations of geometry, boundary conditions and loading. However, several examples have been studied using the program. These examples are believed to represent a class of problems frequently encountered in the analysis of ship structures. It is expected that these examples will demonstrate the effectiveness of the present computer program in solving linear stiffened-plate problems within its range of applicability.

4.3 Comparison Study of Different Membrane Elements

Before proceeding to apply the program to various stiffened plate problems it seemed desirable to make a comparison of the effectiveness of two different types of plate membrane elements -- the ordinary and the constant shear elements as described in Section 2.2. This comparison demonstrated the relative efficiency of these elements in predicting membrane stresses in the plate assemblage. For this demonstration, the problem of local plate-stiffener bending in an orthogonally stiffened plate as described in Section 4.2 and illustrated in Fig. 4.1 was selected. The loading was assumed to be uniform pressure over the plate field of intensity $p = 17.3$ lb/in^2 (equivalent to 40 feet water pressure). An aspect ratio of 2.5 was chosen and the following, geometric parameters were selected:

a_x (spacing between longitudinals) = 30 in.
a_y (spacing between transversals) = 75 in.
t (plate thickness) = 0.375 in.
h_x (height of transversals) = 20 in.
t_x (web thickness of transversals) = 0.625 in.
A_x (top-flange area of transversals) = 5 in.^{2}
h_y (height of longitudinals) = 5 in.
t_y (web thickness of longitudinals) = 0.375 in.
A_y (top-flange area of longitudinals) = 2.2625 in.^{2}

Fig. 4.2 shows three different finite-element meshes which were adopted for this study. The problem was solved using the different meshes and applying the two different membrane elements. Part of the results for membrane stresses of the plating are given in Figs. 4.3 and 4.4 where normal stresses along the edges of a quarter of a plate panel are given*. From these figures it can be seen that at the corner points of the plate panel the values of longitudinal membrane stress and its gradient along the transversals are relatively high. For design purposes it seems particularly important to obtain a good representation for the value of longitudinal stress at these points. A comparison of the results for the different meshes reveals that as finer meshes are used for the problem, higher estimates are obtained for this stress value. The highest estimate ($14895^{lb/in^2}$) was obtained by the mesh Q-48 when using constant shear elements. This value is evidently a lower bound for the true value and can be regarded as the best estimate obtained in this study. It can be seen from the figures that the stress value obtained by the coarse mesh (Q-6) and constant shear elements is closer to the best estimate than that obtained by the fine mesh (Q-48) using ordinary elements. Thus it can be concluded that as far as stiffened plate problems are concerned, the constant shear elements, when used to simulate the membrane behavior of the plating, are much more efficient than the ordinary elements in predicting high stress concentrations. Based on this result it was decided to utilize the constant shear element for all subsequent studies.

4.4 Finite Element Results versus Estimates Based on the Effective Width Concept.

A local plate-stiffener bending problem (see Section 4.2 and Fig. 4.1) was studied in order to make a comparison between finite element stress results

* In all the examples the modulus of elasticity and the Poisson's ratio are assumed to be 3×10^7 lb/in^2 and .3 respectively.

and approximate estimates based on the classical concept of effective width of plating acting as a flange for the stiffeners. An aspect ratio of 5 was chosen and the following parameters were selected:

a_x = 30 in.
a_y = 150 in.
t = .375 in.
h_x = 20 in.
t_x = .625 in.
A_x = 5 in^2
h_y = 18 in.
t_y = .375 in.
A_y = 2.625 in^2

where the different parameters are defined as in Case 4.3. Fig. 4.5 shows two finite element meshes used for this study; only the constant shear element was used in this problem. The results for the normal membrane stresses along the edges of a quarter of the plate panel are shown in Fig. 4.6. As in the case of 4.3, the maximum longitudinal membrane stress was obtained at the corner points of the plate panel. A comparison of the results for two different meshes reveals that even with the coarse mesh a good estimate has been obtained for the longitudinal stress value; the transverse stress is relatively less accurate in the coarse mesh solution, but it also is less significant.

In general, the local plate-stiffener bending problem involves bending of stiffeners in two orthogonal directions. However, in the classical method of analysis, which is valid in the case where the aspect ratio is large, the problem is considered as one in which the bending of stiffeners in one direction only is involved. In fact, it is assumed that the whole lateral pressure is uniformly distributed along the longer edge beams and these beams are clamped at the stiffener intersections. This idealization was made for the present case as shown in Fig. 4.7 where the bending moment diagram along the stiffener

is given. The longitudinal stress of the plating at the center and the ends of the beam was calculated on the basis of effective flange width of the plating, as obtained from the curves given by Schade in Ref. [18]. For this purpose the segment CD (see Fig. 4.7) was idealized as a simply supported beam under action of a uniformly distributed load whereas the segment AC was idealized as a half of a simply supported beam under action of a concentrated load at the middle. The above idealization is suggested by Schade [18] based on the results that he has obtained for effective flange width at different cross sections. Having the effective flange width at the ends and the center of the beam, the corresponding section modulus and longitudinal membrane stress of the plating were calculated.

The results of these calculations are indicated in the Table 4.1. In this table the finite element results for stress value in the plating at the different cross-sections also have been given. The finite element results are compared with approximate stress values obtained on the basis of effective width concept. The percentage difference between results of the two different methods is also indicated in that table. Is is believed that this significant discrepancy is due mainly to the errors involved in calculation of the effective flange width. This judgment has been reached on the basis of the quite close agreement between the results obtained by the finite element method of analysis and a refined analytical solution in the case of a simpler example as described in Section 4.5. It should also be mentioned that the simplification made in the problem by ignoring the bending of transversals cannot result in differences comparable to those indicated in Table 4.1.

Table 4.1. Longitudinal Stresses in Stiffened Plating

Position Along the Stiffener Segment		Middle	Ends
Effective Width/Spacing of Longitudinals		0.90	0.53
Stress Value	Finite Element Method	2960	9397
	Effective Width Concept	2750	8320
Difference		7%	11%

Note: These stresses are computed in a segment of a longitudinal between stiffener intersections, see Fig. 4-7.

4.5 Infinite Plate Strip with Transverse Stiffeners

This example was selected in order to compare the results obtained by the finite element method with results of an analytical solution. A uniform infinite plate strip with an infinite number of transverse stiffeners was examined. A single stiffener and a part of the plating between two successive mid-sections of the plate panels are shown in Fig. 4.8. The stiffeners are assumed to be subjected to uniformly distributed load perpendicular to the plating surface and along the plate-stiffener junctions. The plate-stiffener combination is assumed to be supported along the longitudinal edges in such a way that its lateral deflections and longitudinal displacements are constrained. Along these edges the structure is free to have transverse displacement and rotations about the longitudinal axis. Due to the uniformity of the loading and the structure, at junctions of the plate and stiffeners, and at transverse mid-sections of the plate panels the displacements in the longitudinal direction and the rotations about the transverse axis are

assumed to be constrained by symmetry conditions. All these boundary conditions together with geometric parameters are shown in Fig. 4.8. Due to the symmetries, only a quarter of one plate panel and a quarter of one stiffener was included in the finite element analysis. The finite element idealization for this example is shown in Fig. 4.9 where the letters at the corner points indicate the corresponding points in Fig. 4.8. The finite element program was applied to solve the problem and the results were compared with an analytical solution which has been obtained by H. Payer (*) and is explained very briefly in the following paragraphs.

In the analytical solution the web of the stiffener as well as the plating is treated as an element in a state of plane stress. The top flange is idealized as a bar element, i.e., any shear lag or bending effect in this element is neglected. The equilibrium equations of the plating and the web are satisfied by introducing two Airy stress functions F_i (i = 1, 2 for the plating and the web) such that the membrane stresses of the element i satisfies:

$$(\sigma_x)_i = \frac{\partial^2 F_i}{\partial y^2}$$

$$(\sigma_y)_i = \frac{\partial^2 F_i}{\partial x^2} \qquad i = 1,2 \qquad (4.1)$$

$$(\tau_{xy})_i = -\frac{\partial^2 F_i}{\partial x \partial y}$$

By means of Eqs. 4.1 and the constitutive equations it can be shown that the compatability equations of the plating and the web are satisfied if F_i are solutions of two following biharmonic equations:

$$\nabla^4 F_i = 0 \qquad i = 1,2 \qquad (4.2)$$

(*) Graduate Student at Naval Architecture, University of California Berkeley, California

Eqs. 4.2 are solved by separation of variables; the results for the case of simply supported edges are written in the following form:

$$F_i = \sum_{n=1,\ 3,\ 5\ \ldots}^{\infty} \sin \omega_n y \ (A_i + C_i \omega_n x_i) \cosh \omega_n x_i + (B_i + D_i \omega_n x_i) \sinh \omega_n x_i \quad (4.3)$$

where $\omega_n = \frac{n\pi}{L}$ (L is length of the stiffener.) $x_1 = x$ and $x_2 = z$.

The unknown coefficients in Eq. 4.3 are evaluated by means of the specified boundary conditions as well as compatibility and equilibrium requirements along the element junctions. The boundary conditions are exactly the same as shown in Fig. 4.8 and explained earlier in this section. However, displacement boundary conditions should be first interpreted in terms of stresses before evaluation of unknown coefficients in Eq. 4.3. The analytical solution of the problem has been obtained by using eleven terms of each stress function which is in the form of an infinite series. Part of the results obtained for membrane stresses of the plating and the flange by the finite element method and this analytical method are shown in Figs. 4.10 and 4.11. The results are generally in good agreement; especially for the large membrane stresses of the plating along the center line of the stiffened plate, very close results have been obtained by the two different methods.

An additional example also was studied which, except for the boundary conditions, was similar in all details to the previous one. In this example, at both edges of the plate strip in-plane displacements were allowed while lateral deflection was constrained. The finite element program was applied to the problem using two different meshes. One mesh was identical to that used in the previous study (Fig. 4.9); the other had the same number of elements as the first; however, on the x-axis, its three subdivisions adjacent

to the stiffener were smaller than those adjacent to the center line of the plate panel. The finite element results for the stress distribution of the plate and stiffener were, in general, very close to the results obtained in previous study. However, at the very ends of the stiffener locally high values of σ_x were obtained for the plate. These stress values were -1891 lb/in^2 and -2182 lb/in^2 respectively for the uniform and non-uniform meshes. By studying the in-plane displacements of the plate it can be seen that the elimination of shear strains along the edges of the plate requires compression of the plate at the ends of the stiffener. On the other hand, it can be shown that the points of the plate at the ends of the stiffener are singular and a stress discontinuity exists at these points. In fact, according to Fig. 4.10, the compatibility of the plate and the stiffener requires increasing of the shear stress along their junction towards the edges and this is inconsistent with vanishing of shear stress at the edges. On the basis of the above considerations, no attempt was made to predict the exact stress distribution of the plating in the vicinity of these singular points. However the high σ_x values at these points are a very localized feature and the singularity of these points does not affect the finite element results obtained for adjacent points.

4.6 Simply Supported Plate with Two Orthogonal Stiffeners

Fig. 4.12 shows a simply supported square plate with two identical stiffeners in the x and y directions. Along the edges, the in-plane displacements of the plate are allowed. The stiffened plate is assumed to be subjected to a uniform pressure with intensity of 10 lb/in^2. Three different finite element meshes were selected for this example as shown in Fig. 4.12. The results of the finite element program for the lateral deflections of the

stiffened plate and the membrane stresses of the plating along the half of a center line are shown in Figs. 4.13 and 4.14. It can be seen from Fig. 4.14 that along a stiffener and in its direction the membrane stress of the plating does not have its maximum value at the center of the system. This result which is in contrast with what normally would be expected is due to the shear lag effect in the plating. Another interesting result of the study is that at the ends of a stiffener and in the direction perpendicular to it the value of plate membrane stress is relatively high. This result is consistent with that obtained in Section 4.5 for an infinite plate strip with free ends. For the same reasons as described in Section 4.5, these points are singular and there exists stress discontinuities at these points.

Although an analytical solution of this problem is not available, the example indicates the capability of the program in analyzing a general case in which interaction between plating and stiffeners in two distinct directions is involved.

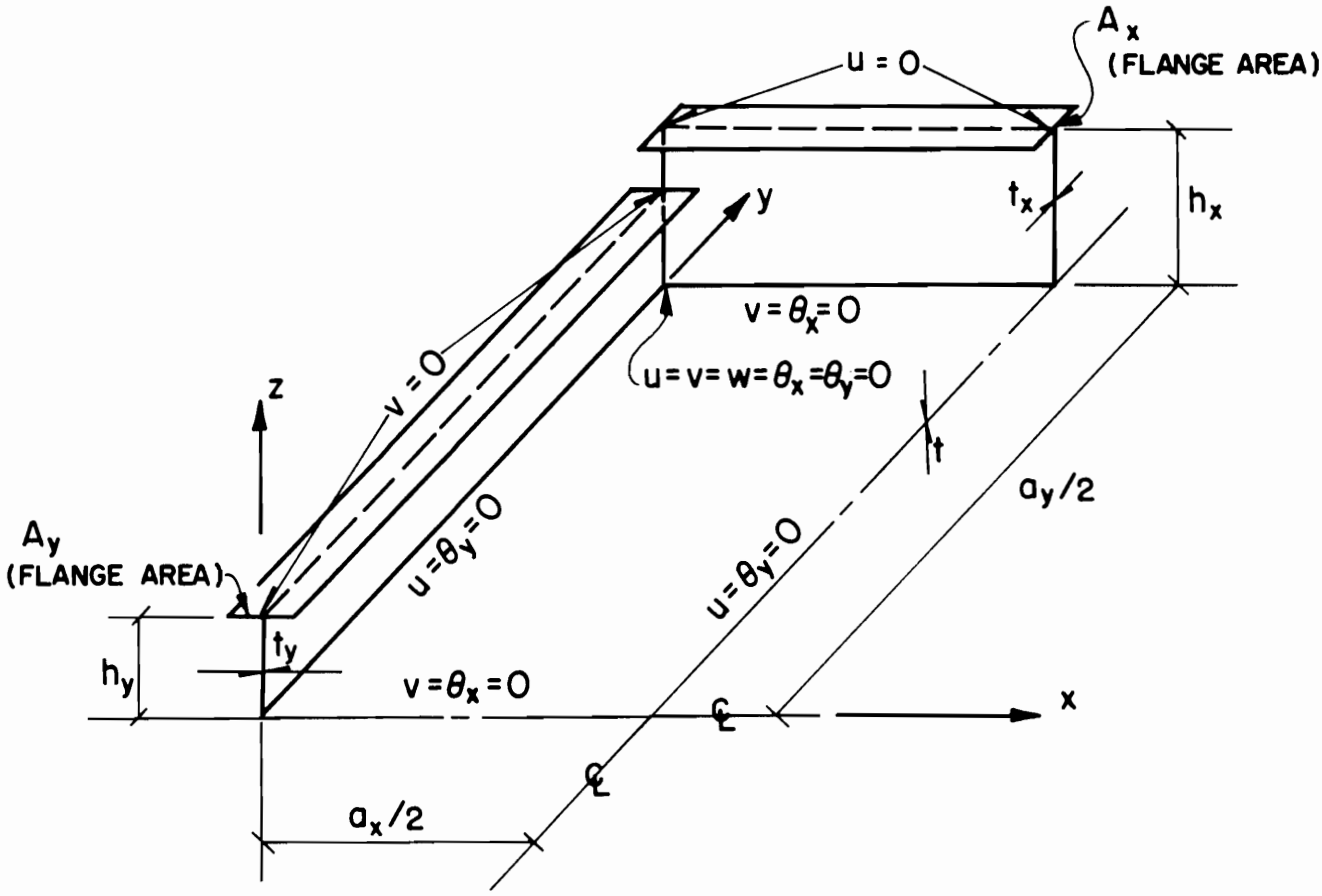

FIG. 4.1 BOUNDARY CONDITIONS FOR LOCAL BENDING OF PLATE STIFFENER SYSTEM

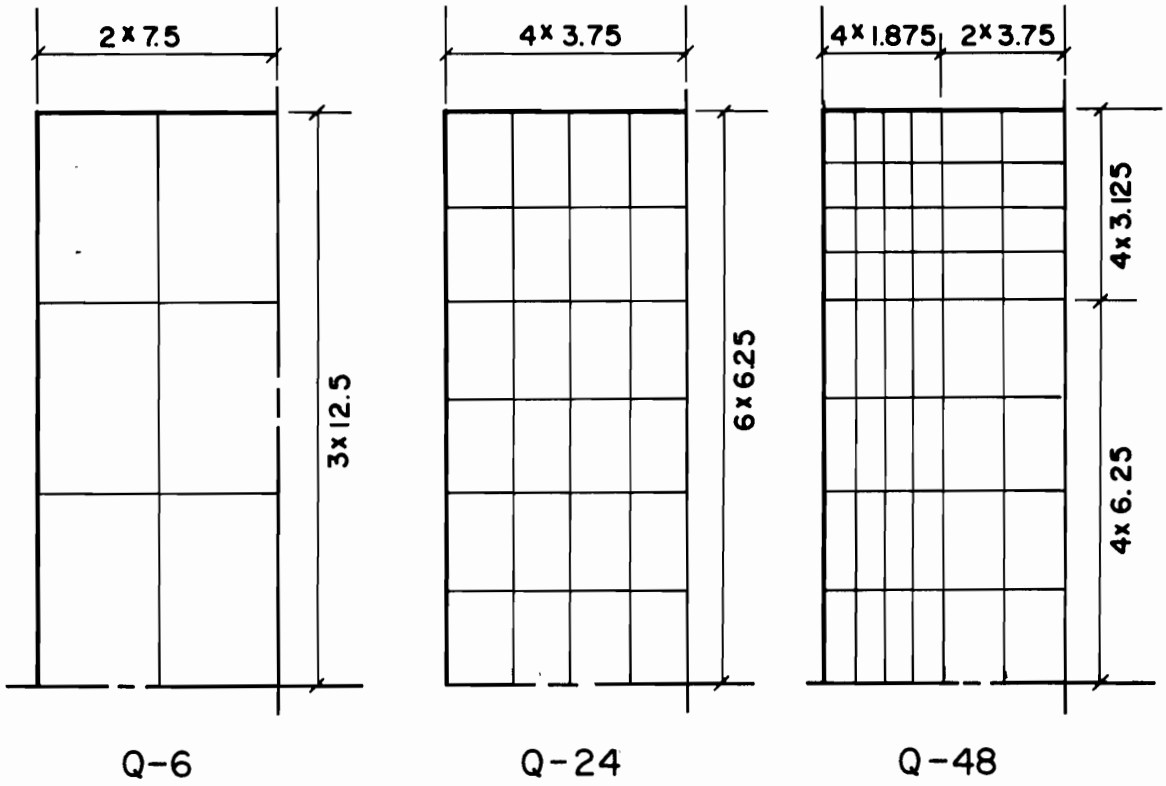

FIG. 4.2 FINITE ELEMENT MESHES FOR QUARTER OF THE PLATE PANEL (SECTION 4.3)

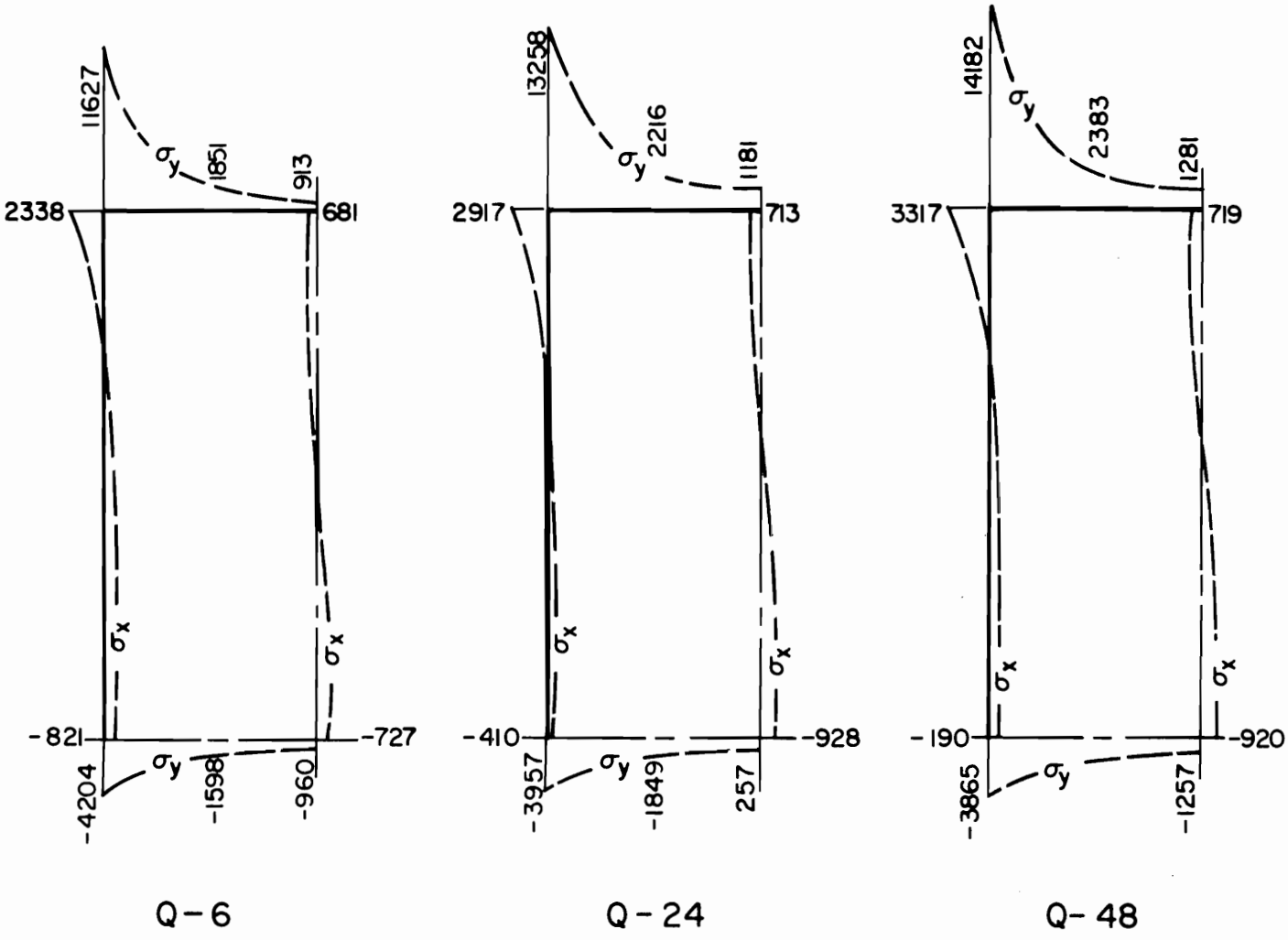

FIG. 4.3 MEMBRANE STRESSES OBTAINED BY ORDINARY ELEMENTS (SECTION 4.3), p = 17.3 LB./IN.^{2}

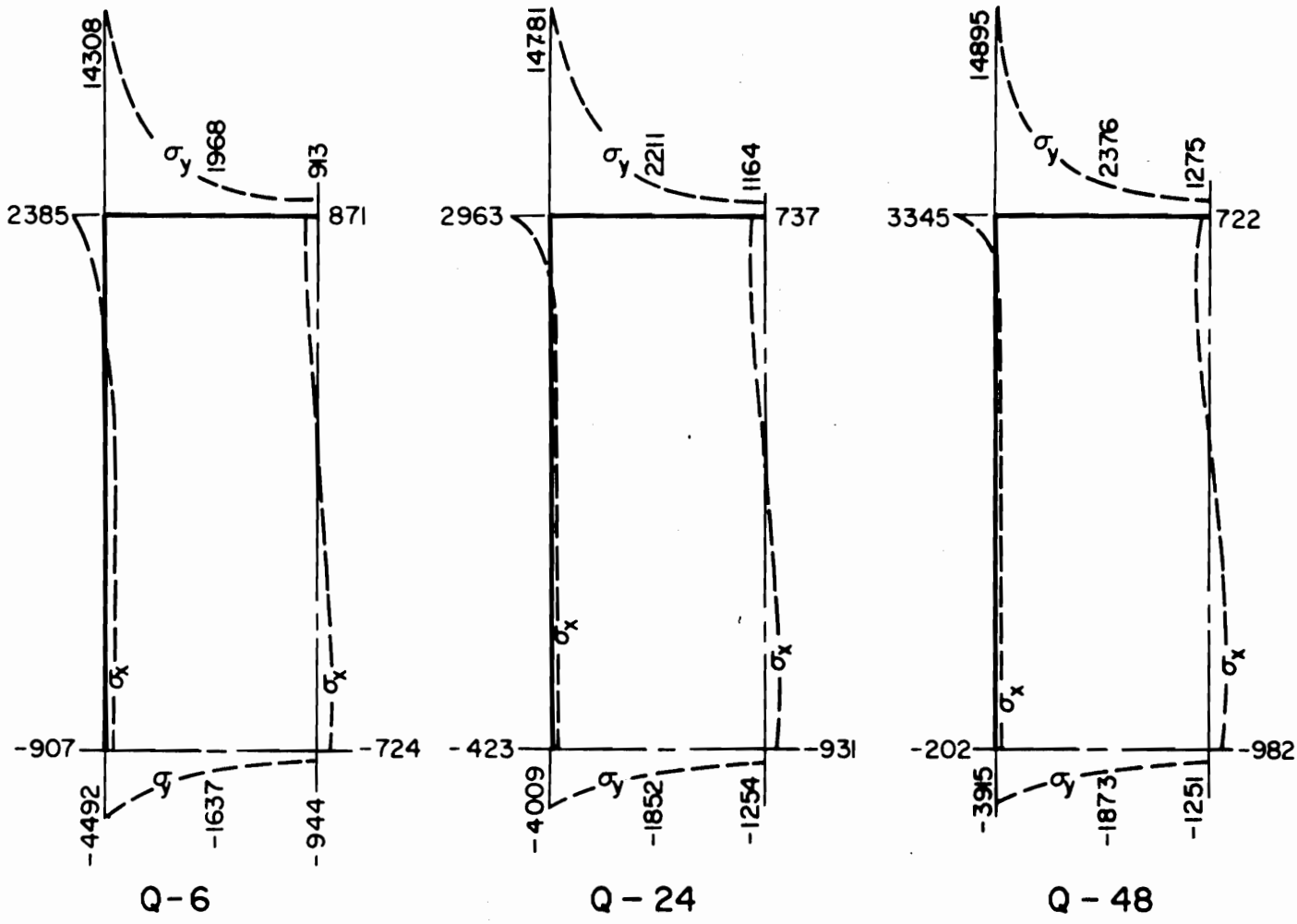

FIG. 4.4 MEMBRANE STRESSES OBTAINED BY CONSTANT SHEAR ELEMENTS (SECTION 4.3), p = 17.3 LB./IN.^{2}

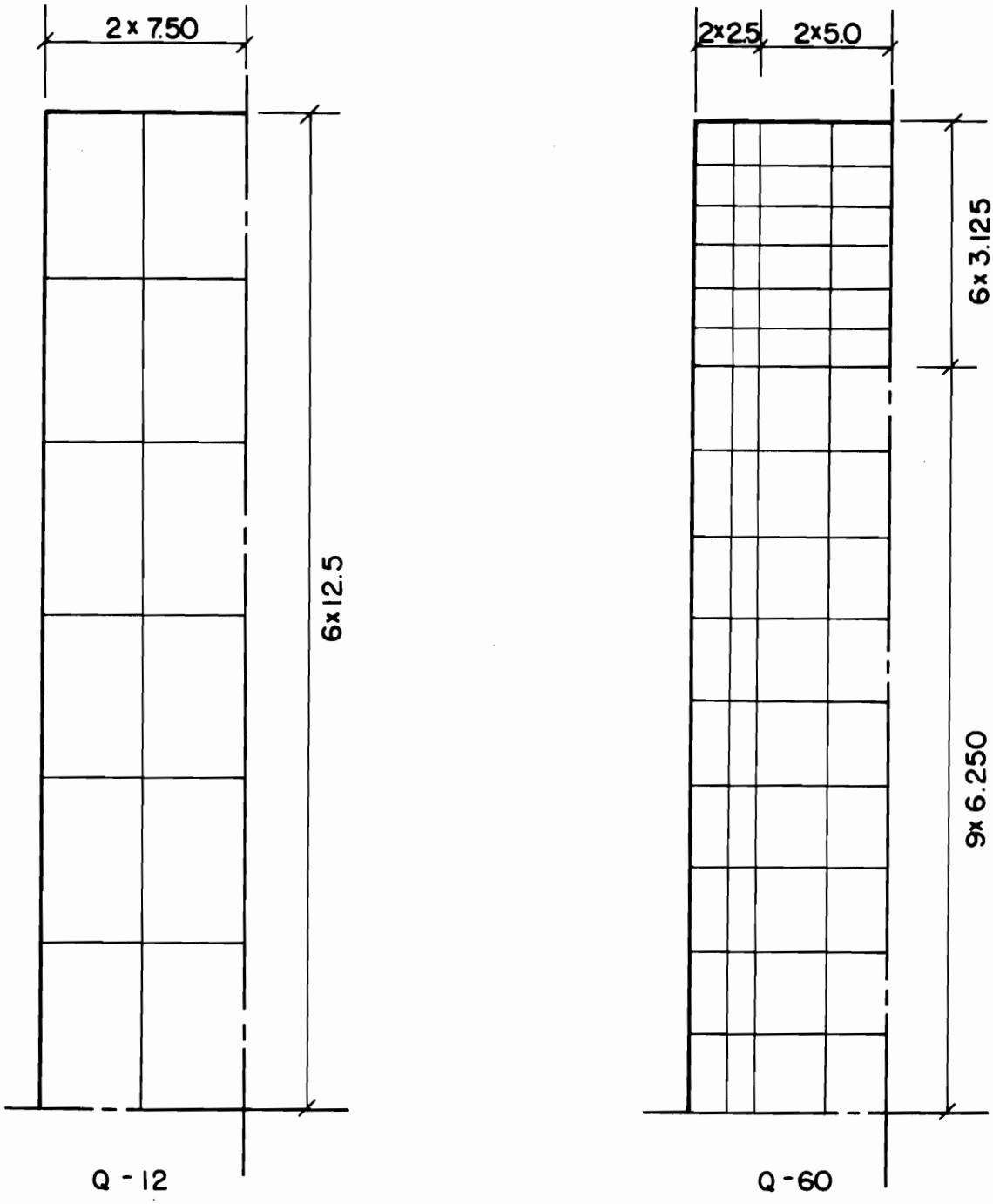

FIG. 4.5 FINITE ELEMENT MESHES FOR QUARTER OF THE PLATE PANEL, (SECTION 4.4)

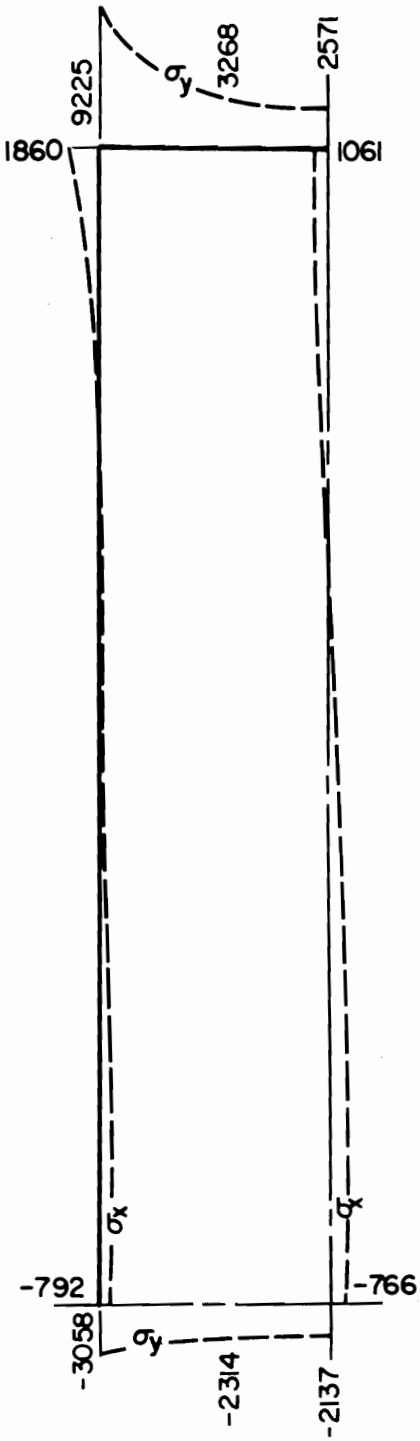

Q-12

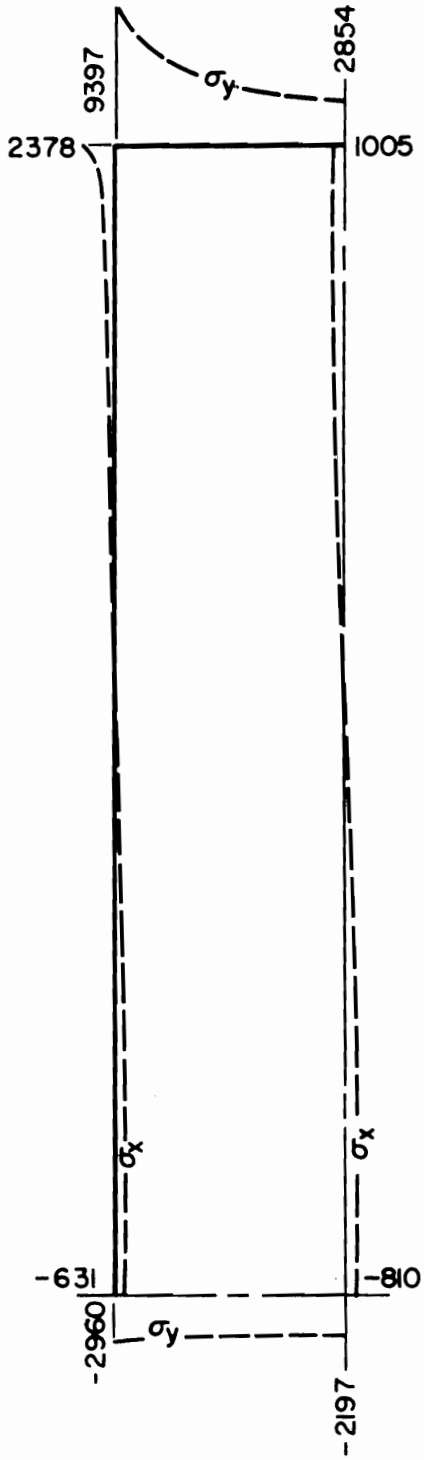

Q-60

FIG. 4.6 MEMBRANE STRESSES (SECTION 4.4), $p = 17.3$ LB./IN^2

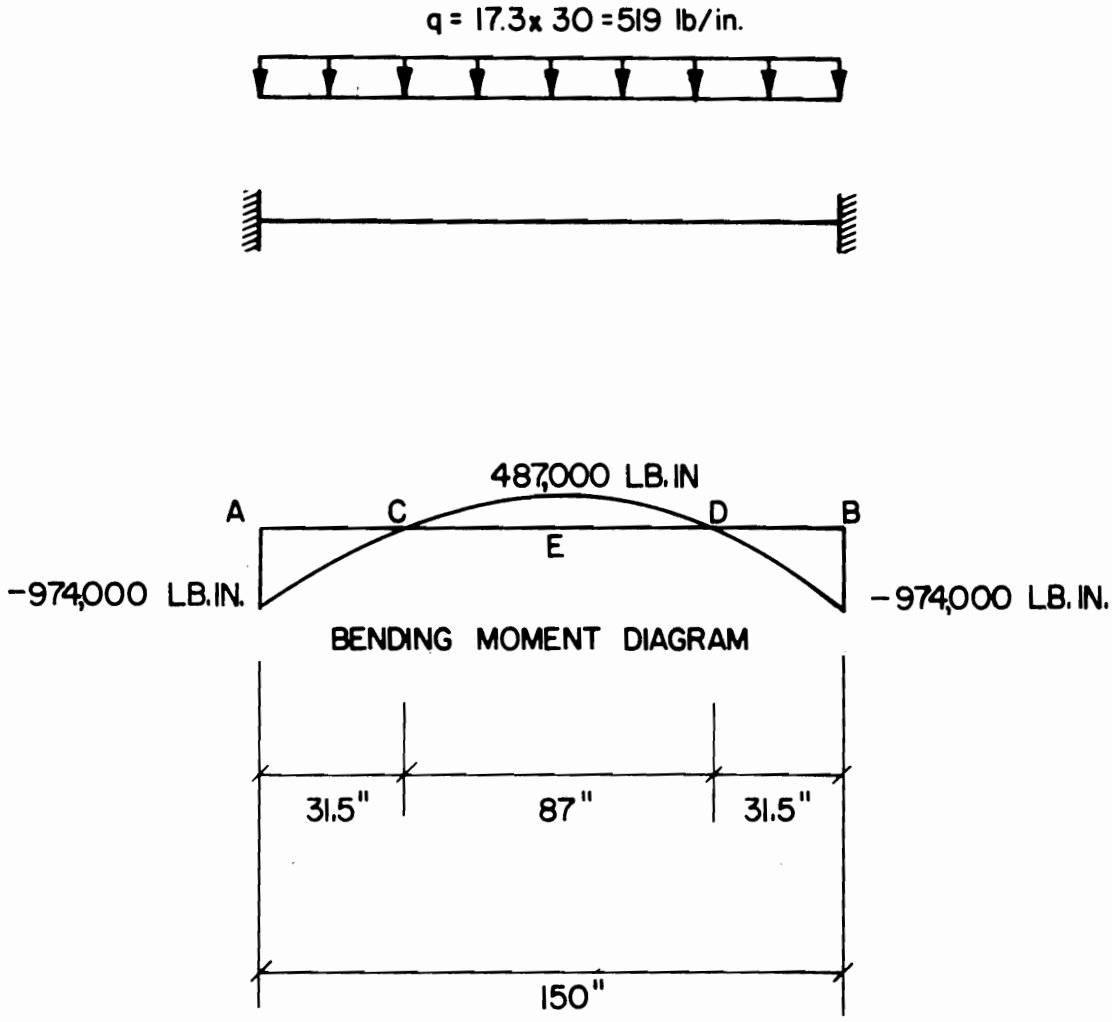

FIG. 4.7 A SEGMENT OF A LONGITUDINAL STIFFNER IDEALIZED AS A CLAMPED BEAM UNDER UNIFORM LOAD

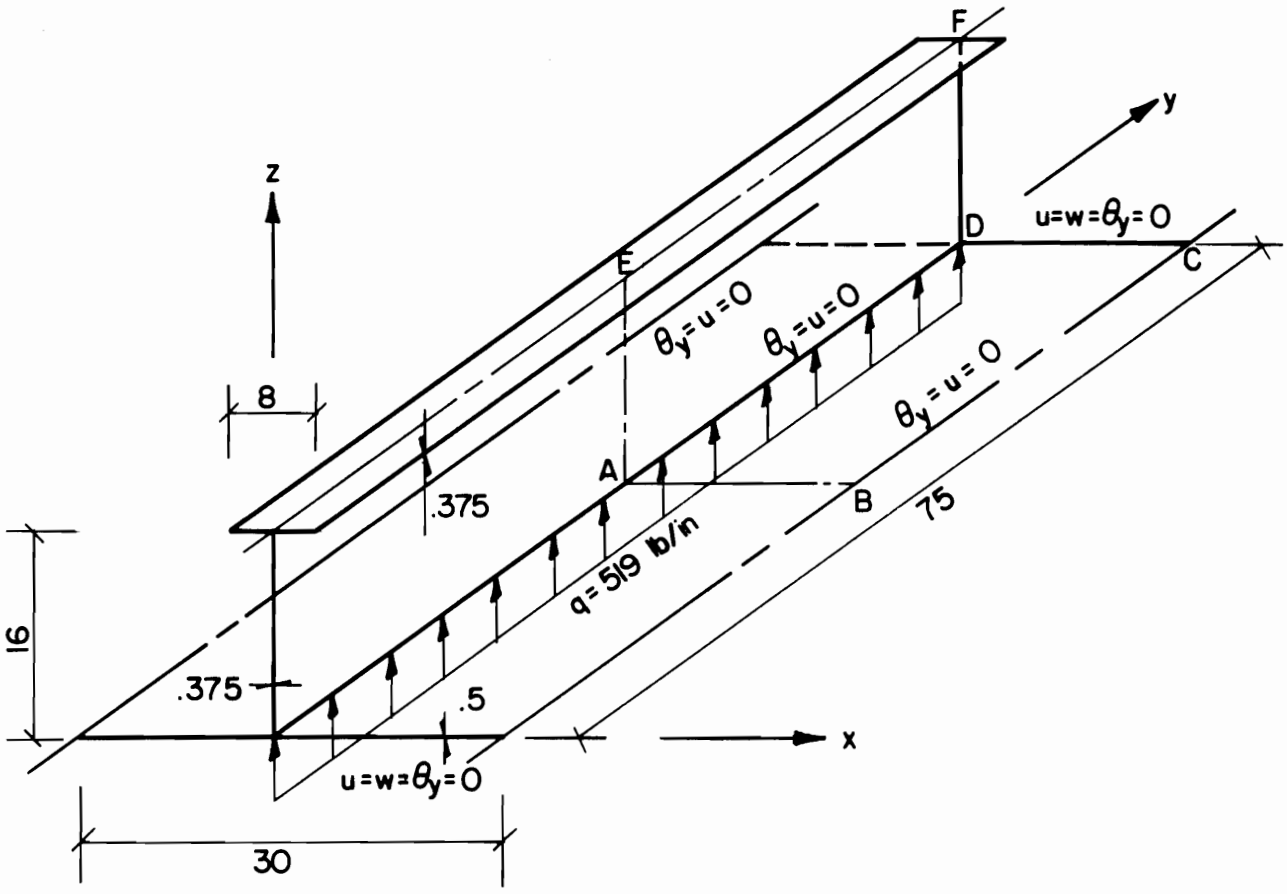

FIG. 4.8 PART OF THE INFINITE PLATE STRIP STIFFENED WITH TRANSVERSE STIFFENERS (SECTION 4.5)

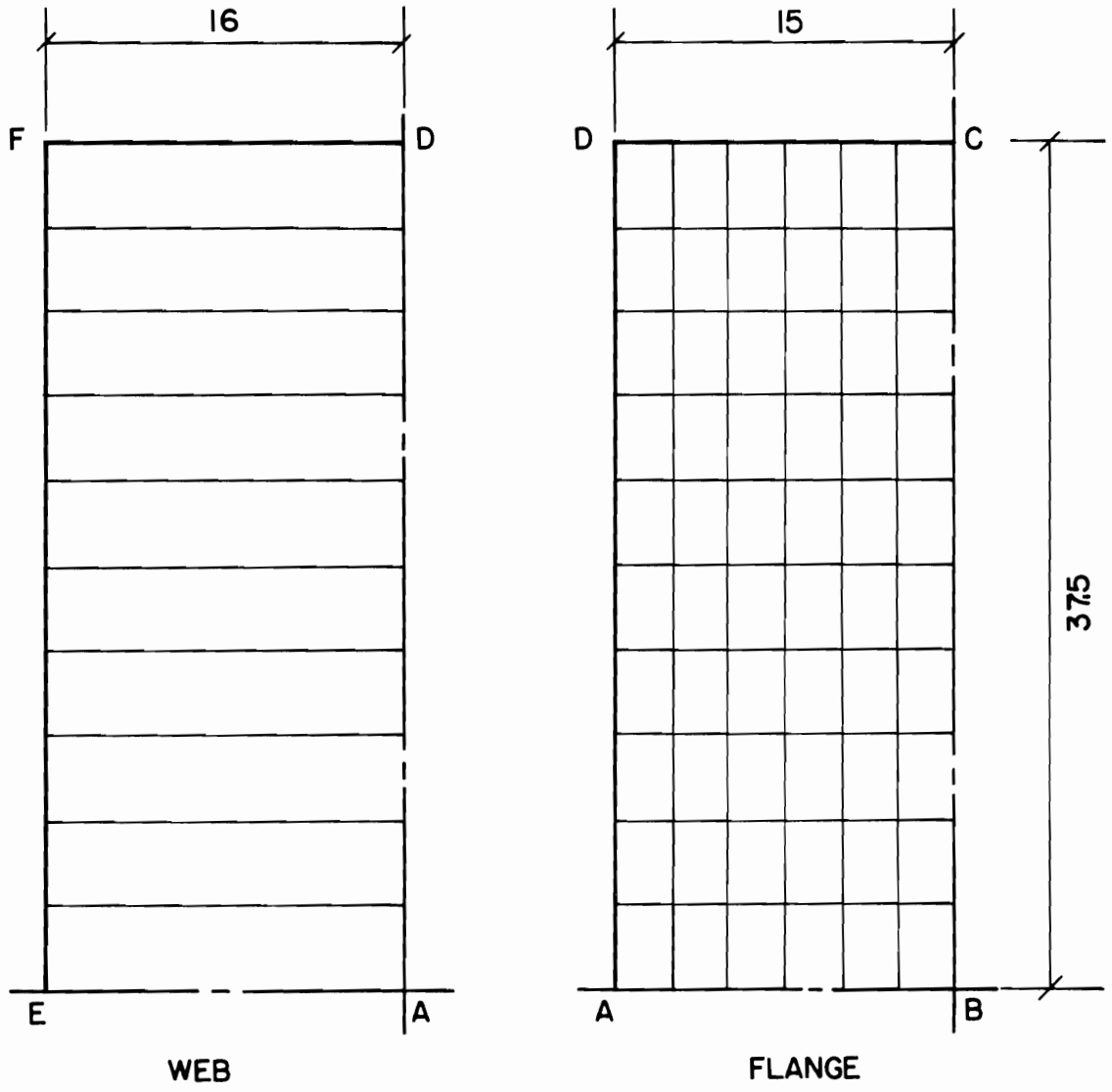

FIG. 4.9 FINITE ELEMENT MESH USED IN THE EXAMPLE OF SECTION 4.5

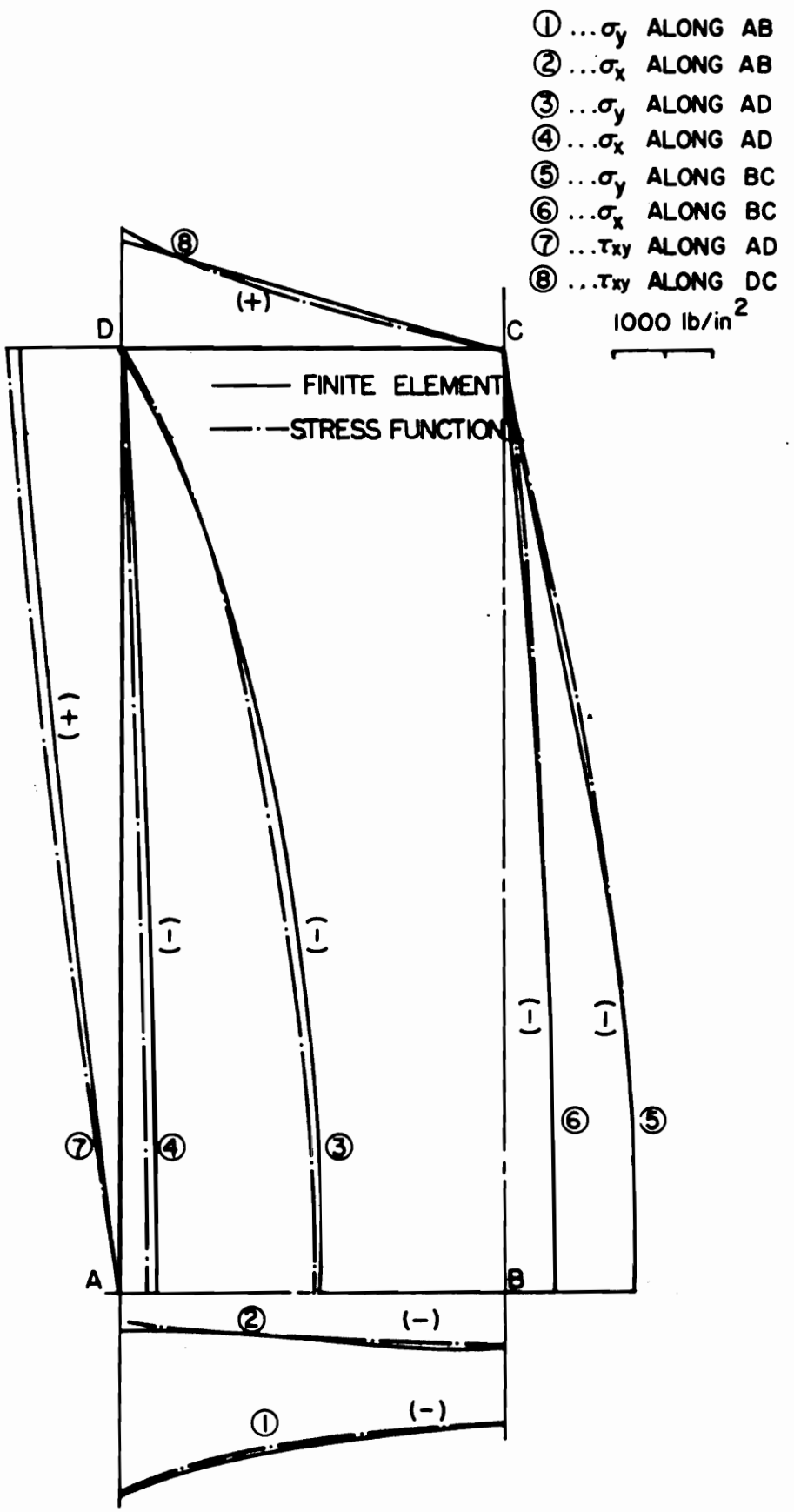

FIG. 4.10 MEMBRANE STESSES OF THE PLATE, EXAMPLE OF INFINITE PLATE STRIP

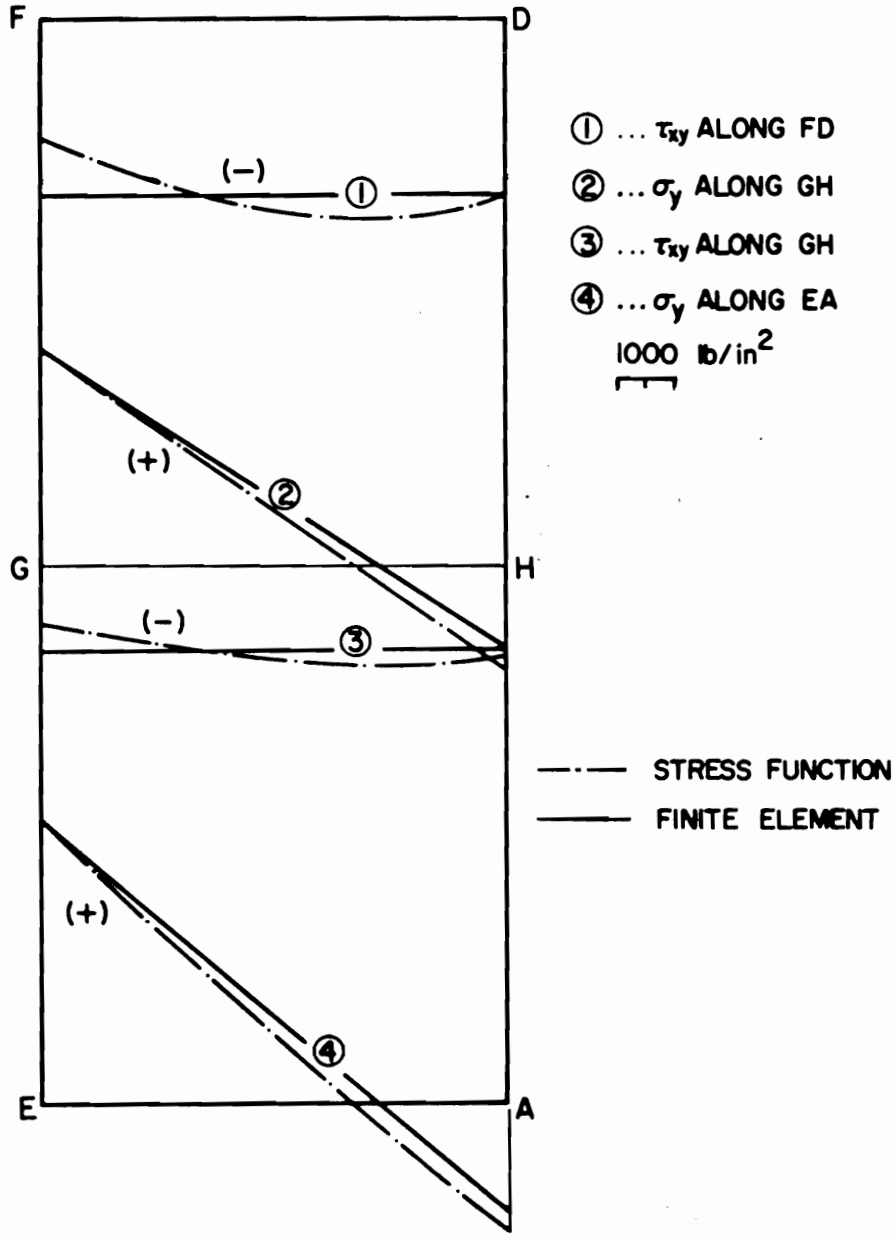

FIG. 4.11 MEMBRANE STRESSES OF THE WEB, EXAMPLE OF INFINITE PLATE STRIP

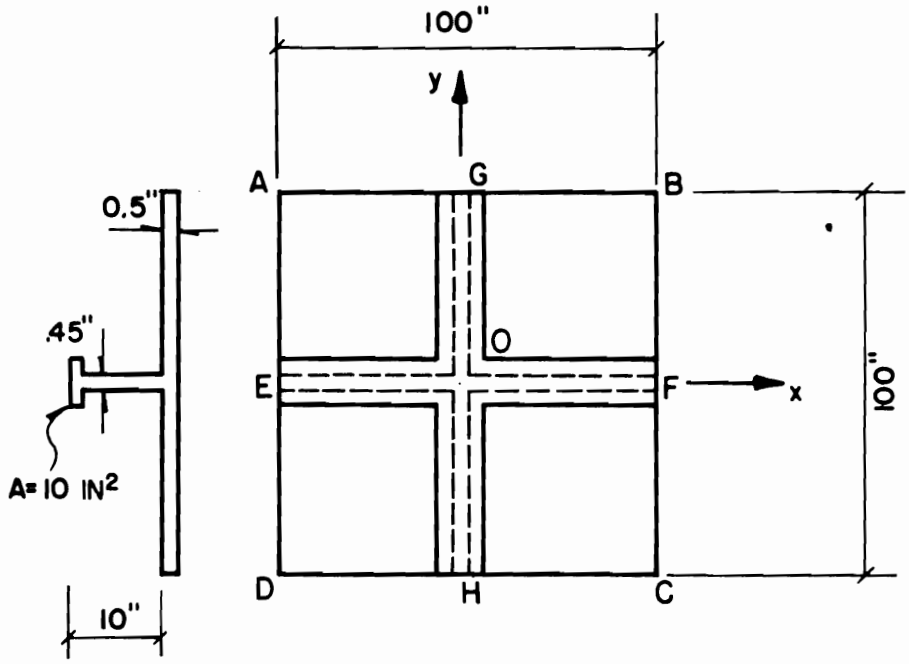

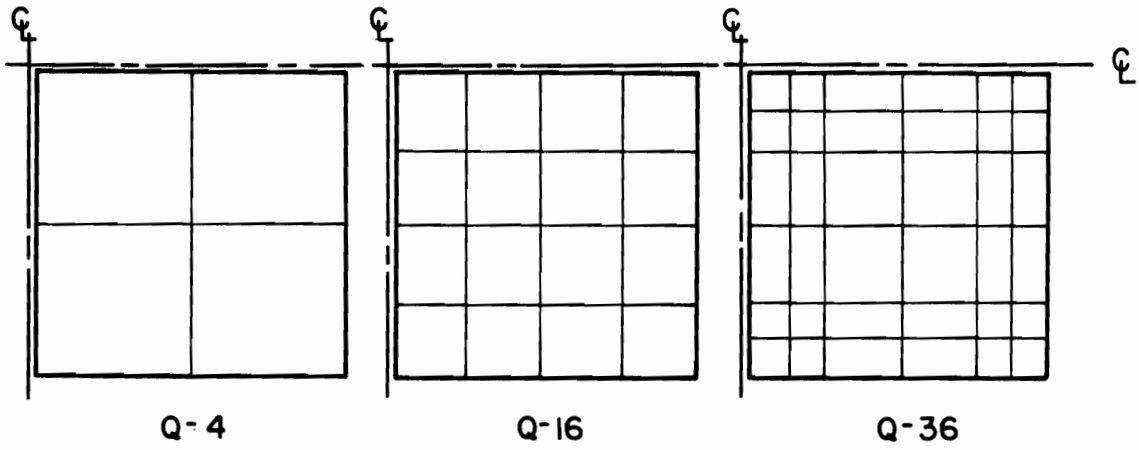

FIG. 4.12 SIMPLY SUPPORTED STIFFENED PLATE AND THE FINITE ELEMENT MESHES (SECTION 4.6)

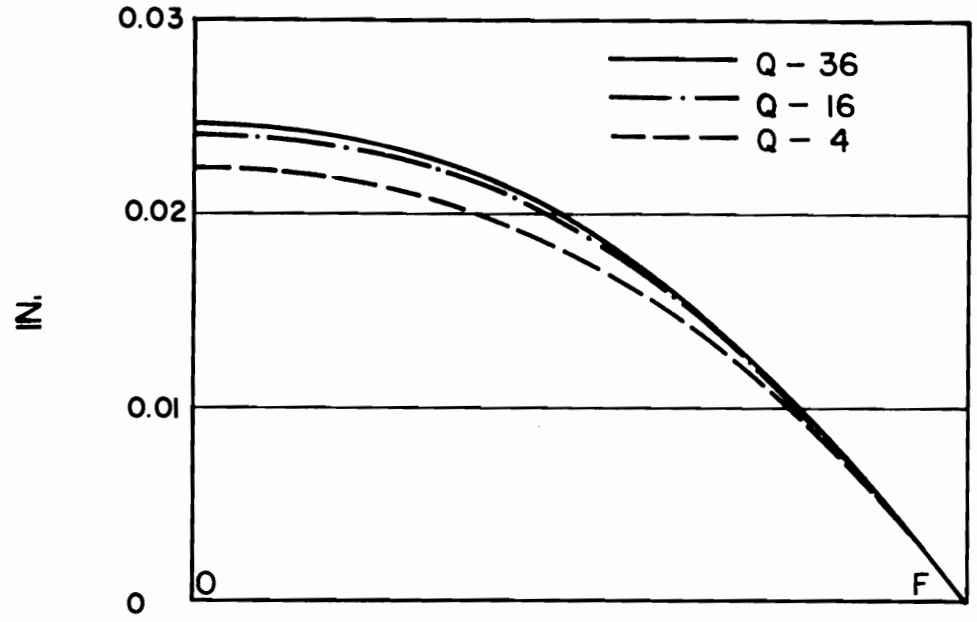

FIG. 4.13 DEFLECTIONS ALONG HALF OF A CENTER LINE (SEE FIG. 4.12)

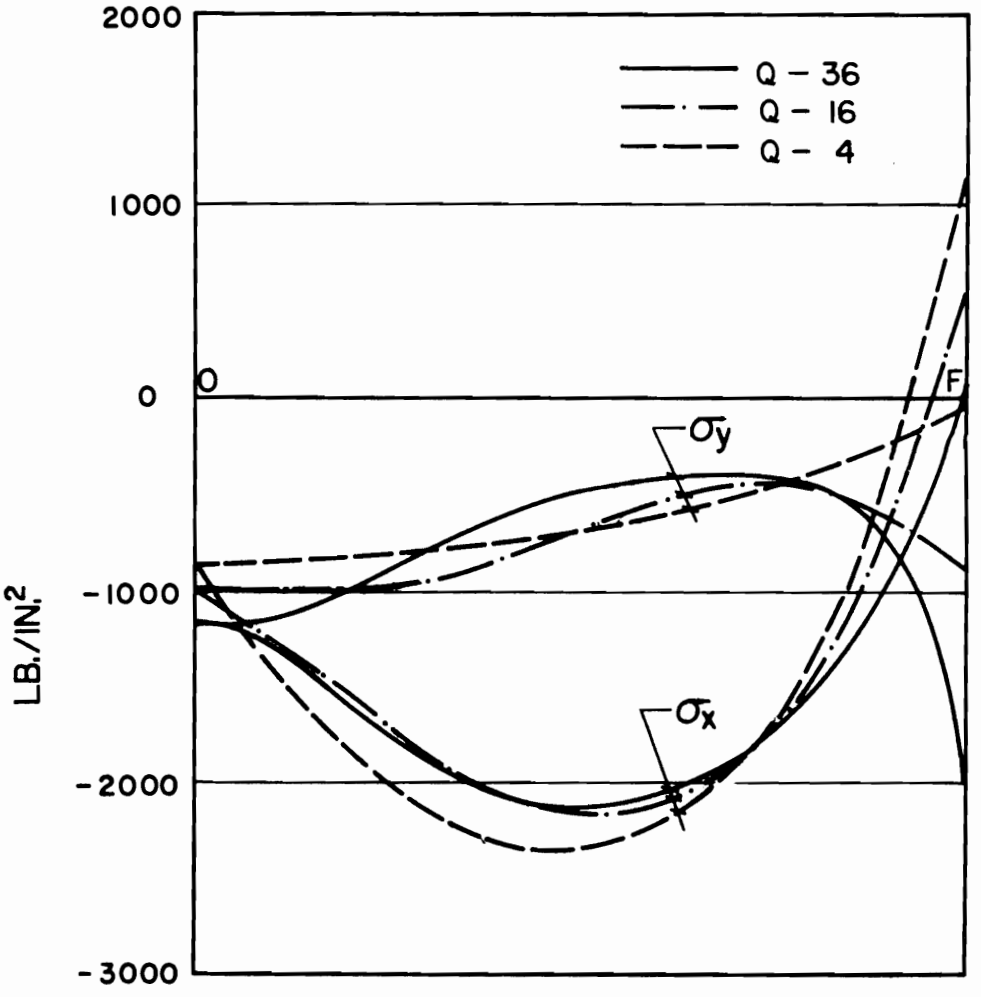

FIG. 4.14 MEMBRANE STRESSES OF THE PLATING ALONG HALF OF A CENTER LINE (SEE FIG. 4.12)

5. DESIGN CURVES FOR LOCAL PLATE-STIFFENER BENDING

When an orthogonally stiffened plate is subjected to uniform lateral pressure, significantly high stresses may be induced in the plating due to the sagging of stiffeners between intersection points. In general, these stresses are influenced by the stiffness properties of both sets of longitudinal and transverse stiffeners. However, in practical cases, the transversals are much stronger than the longitudinals in withstanding lateral loads. Therefore, these local membrane stresses of the plating are mostly due to the local sagging of the longitudinal stiffeners.

As observed in sections 4.3 and 4.4, the maximum principal stress of the plating due to the local plate-stiffener bending occurs at the corner points of the plate panel. For design purposes it seemed desirable to study the effect of different geometric parameters on this stress value. For this purpose certain ranges for the geometric parameters were assumed. These ranges are shown in Table 5.1 and are believed to cover most cases of practical interest in the design of ship-bottom structures. A number of different cases were studied using the finite element program. The dimensions in each case were within the assumed ranges and were such that reasonable proportions were obtained for the structure. By means of systematic geometric variations and on the basis of computer results, a set of curves were prepared which can be used to estimate the maximum longitudinal membrane stress of the plating with an error less than 4%. It is hoped that these curves may be useful in estimating the maximum principal stress in the plating at the early design stages. If necessary a better estimate can be obtained at any time using the program and a fine mesh.

Table 5.1: "Ranges of Different Geometric Parameters Assumed in Preparation of the Design Curves"

Geometric Parameter		Range (in. or $in.^2$)
Symbol	Description	
a_x	Spacing between longitudinals	18-36
a_y	Spacing between transversals	60-300
t	Plate thickness	5/16-$\frac{1}{2}$
h_x	Height of transversals	20-38
t_x	Web thickness of transversals	7/16-7/8
A_x	Top-flange area of transversals	2.2-8.8
h_y	Height of longitudinals	6-18
t_y	Web thickness of longitudinals	$\frac{1}{4}$-7/16
A_y	Top-flange area of longitudinals	1-4

A quarter of a plate panel with appropriate parts of the surrounding beams (see figure 4.1 and footnote on page 41) were included in the finite element analysis. The finite element mesh for the one-quarter plate panel consisted of 2 elements in the transverse direction and from 3 to 8 elements, depending on the aspect ratio, in the longitudinal direction. Using such a mesh, it is possible to predict the longitudinal stress at the corner points with an error less than 4%. This error, as can be seen from the results represented in the sections 4.3 and 4.4, is significantly influenced by the aspect ratio. It is approximately equal to 4% and 2% for the aspect ratios equal to 2.5 and 5 respectively.

As was mentioned earlier, the effect of local bending of transversals, in general, is much smaller than that of longitudinals. This means that

the cross-sectional dimensions of the transversals do not significantly influence the stress distribution of the plate panels. The validity of this assumption was examined for the ranges of parameters adopted for this study by means of a few examples. In fact, it was found that the effect of transversals were quite negligible when compared with those of longitudinals. Two examples have been given in table 5.2 where σ_x and σ_y are the membrane stresses at the corner points of a plate panel due to lateral pressure of intensity p over the plate field.

Table 5.2: "Examples Showing the Effect of Transversals on the Stresses of Intersection Points Due to the Local Bending."

Example	a_x	a_y	t	h_x	t_x	A_x	h_y	t_y	A_y	σ_x/p	σ_y/p
1	20	40	.375	15	0.50	4	6	0.25	1	43.9	221.5
2	20	40	.375	6	.250	1	6	.25	1	47.6	220.8

Some of the dimensions in these two examples were selected out of the assumed range in order to amplify the effect of transversals on the membrane stresses. For instance, the aspect ratio in these examples is smaller than those normally given by Table 5.1. Obviously, for aspect ratios greater than 2, the membrane stresses will be much less sensitive to any change in the cross-sectional dimensions of the transversals. Moreover, the sizes of transversals in these examples are smaller than those given

in Table 5.1, therefore the effect of transversals on the membrane stresses is more significant than what it normally is in practice. Still the membrane stresses are very insensitive to changes inthe geometry of transversal cross-sections.

On the basis of the above considerations, a fixed transversal geometry (h_x = 20 in., t_x = 0.45 in., A_x = 2 in.^{2}) was selected for all subsequent cases and membrane stresses were assumed to be mainly due to the sagging of the longitudinals between the stiffener-intersections.

In order to have a basis for the recognition of the different factors influencing the masimum principal stress it is suitable to visualize the longitudinal as an element which includes an effective width of plating as its flange. This beam is clamped at the ends and it is under action of uniform load, transmitted to it by the plating.

The lateral load on the beam, in general, is not known but it has been found [5] that the proportions of total load carried by each set of stiffeners depend mostly on the aspect ratio $\lambda = \frac{a_y}{a_x}$ and is not significantly affected by stiffness properties of the stiffeners. On this basis, the bending moment at the ends of the idealized beam can be written:

$$M = f(\lambda)\ p a_x\ a^2{}_y/12 \qquad (5.1)$$

where p is intensity of the lateral pressure and f is a function which represents the effect of aspect ratio on the distribution of the field pressure over the stiffener.

If a_x is the effective flange width and S_y is the section modulus of the beam element at the corner points of the plate panel, the longitudinal stress at these points can be written:

$$\sigma_y = \frac{M}{S_y} = \frac{M}{{}^2/_3 \, a_x \, a_y^2 \, \Phi \left(\frac{\bar{a}_x}{a_x} + \frac{\Psi}{4} \right)} \tag{5.2}$$

where $$\Phi = h_y t \left(\frac{3 A_y + h_y t_y}{2 A_y + h_y t_y} \right) \Big/ a^2_y \tag{5.3}$$

and $$\Psi = \frac{h_y t_y}{a_x t} \left(\frac{4A_y + h_y t_y}{3A_y + h_y t_y} \right) \tag{5.4}$$

An analytical treatment of the effective flange width problem by Schade has revealed that the dimensionless quantity $\frac{\bar{a}_x}{a_x}$ depends on the aspect ratio λ and the parameter Ψ. On this basis and by combining Eqs. 5.1 and 5.2, the stress value can be written as:

$$\sigma_y = \frac{p}{\Phi} \; F(\Psi, \lambda) \tag{5.5}$$

where F is a function of Ψ and λ only. Then the dimensionless parameter $\bar{\sigma}_y = \frac{\Phi \sigma_y}{p}$ can be written as

$$\bar{\sigma}_y = F(\Psi, \lambda) \tag{5.6}$$

On the basis of Eq. 5.6 and the results of the computer program for a number of suitable cases a set of five design curves corresponding to five different values of Ψ were prepared. These curves are shown in Fig. 5.1. They were checked by several examples. In each case the stress value as obtained by the finite-element program was compared with that obtained by using the stress curves. The difference in all cases was less than 2% and it is believed that most of the error arises in interpolation between different curves.

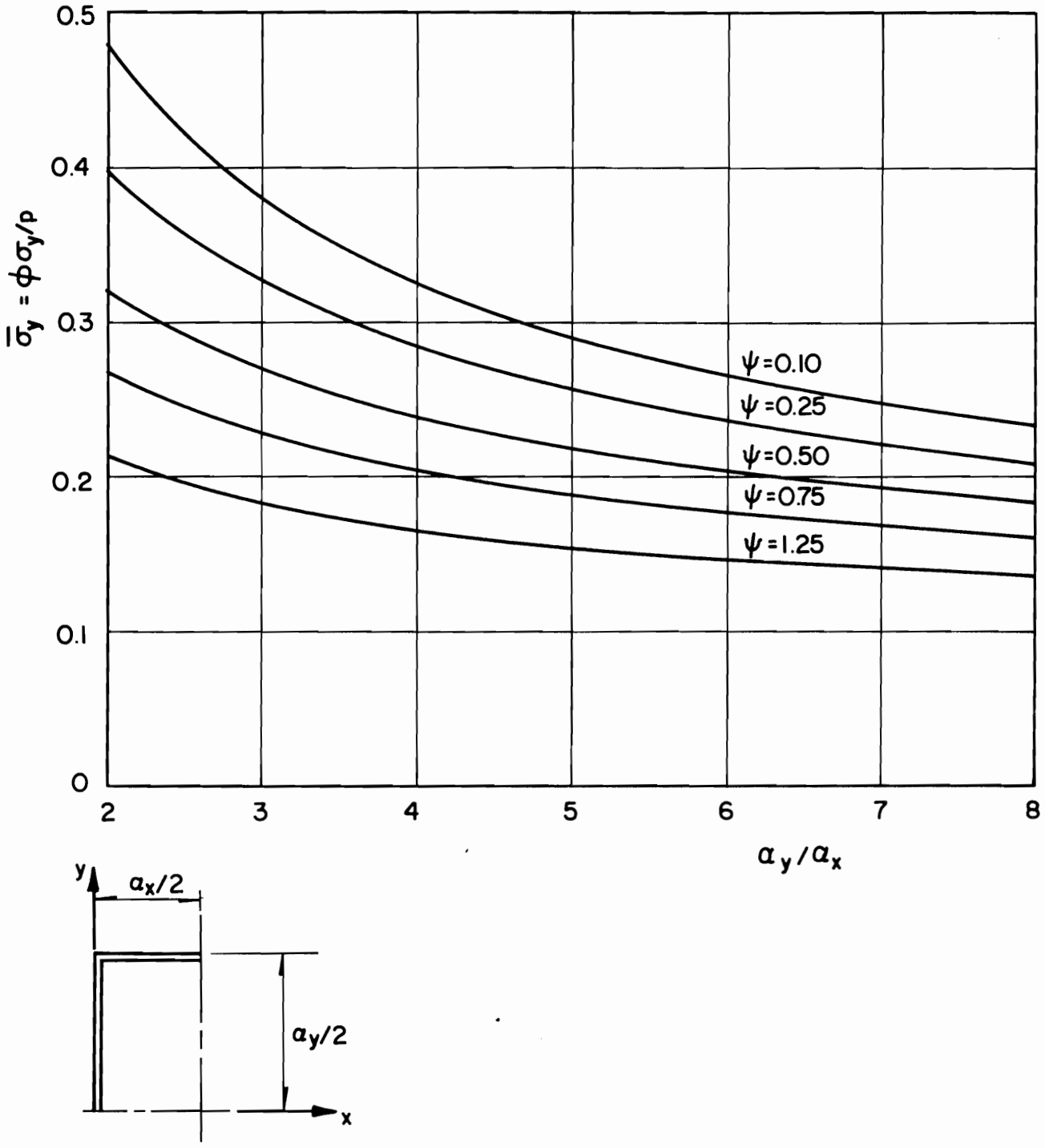

FIG. 5.1 DESIGN CURVES FOR LONGITUDINAL STRESS OF PLATING AT INTERSECTIONS OF STIFFNERS (SEE SECTION 5)

6. REFERENCES

1. Argyris, J.H., Kelsey, S. and Kamel, H., "Matrix Methods of Structural Analysis," AGARD-ograph 72, Pergamon Press, 1963.

2. Clarkson, J., "Tests of Flat Plated Grillages under Concentrated Loads," TRANS.R.I.N.A., 1959, p.129.

3. Clarkson, J., "The Behavior of Deck Stiffening under Concentrated Loads," TRANS. R.I.N.A., 1962, p.57.

4. Clarkson, J., "Tests of Flat Plated Grillages under Uniform Pressure," TRANS.R.I.N.A., 1963, p.467.

5. Clarkson, J., "The Elastic Analysis of Flat Grillages," Cambridge University Press, 1965.

6. Clough, R.W., and Tocher, J.L., "Finite Element Stiffness Matrices for the Analysis of Plate Bending. Proc. 1st Conf. on Matrix Methods in Structural Mechanics, Wright Patterson Air Force Base, Ohio, Oct. 1965.

7. Clough, R.W., and Felippa, C.A., "A Refined Quadrilateral Element for Analysis of Plate Bending," Proc. 2nd Conference on Matrix Methods in Structural Mechanics, Wright Patterson Air Force Base, Ohio, Oct. 1968.

8. Doherty, W.P., Wilson, E.L. and Taylor, R.L., "Stress Analysis of Axi-symmetric Solids Utilizing Higher-Order Quadrilateral Elements," Report No. 69-3, Structural Engineering Laboratory, University of California, Berkeley, California, January 1969.

9. Felippa, C., "Refined Finite Element Analysis of Two-Dimensional Structures, Section II - Plate Bending Problems, Thesis, University of California, Berkeley, 1966.

10. Holand, J., and Bell, K. (editors), "Finite Element Methods in Stress Analysis," Tapir, Trondheim, Norway 1969.

11. Second International Ship Structures Congress, "Report of Committee 3b on Orthogonally Stiffened Plates," Delft, 1964.

12. Mehrain, M., "Finite Element Analysis of Skew Composite Girder Bridge," Ph.D. Dissertation, Dept. of Civil Engineering, Univ. of California, Berkeley, California 1967.

13. Mansour, A.D., "Orthotropic Bending of Ship Hull Bottom Plating under the Combined Action of Lateral and In-Plane Loads," University of California, Report No. NA-66-2, 1966.

14. Przemieniecki, J.S., "Theory of Matrix Structural Analysis," McGraw-Hill 1968.

15. Sanders, G., Beckers, P. and Nguyen, H.D., "Digital Computation of Stresses and Deflections in a Box Beam. A Performance Comparison between Finite Elment Models and Idealization Patterns, Annual Summary, Facultee de Sciences Appliquee, Universite de Liege, Belgium (1966)

16. Schade, H.A., "Bending Theory of Ship Bottom Structures," TRANS. S.N.A.M.E. 1938, Vol. 46..

17. Schade, H.A., "The Orthogonally Stiffened Plate Under Uniform Lateral Load," TRANS. S.N.A.M.E. 1940, Vol. 62.

18. Schade, H.A., "The Effective Breadth of Stiffened Plating under Bending Loads," TRANS. S.N.A.M.E. 1951, Vol. 59.

19. Schade, H.A., "The Effective Breadth Concept in Ship-Structure Design," TRANS.S.N.A.M.E. 1953, Vol. 61.

20. Turner, M.J., Clough, R.W., Martin, H.C. and Topp, L., "Stiffness and Deflection Analysis of Complex Structures," Journal Aero Science, Vol. 23, No. 9, Sept. 1956.

21. "A Guide for the Analysis of Ship Structures," U.S. Department of Commerce, Office of Technical Services, 1961.

22. Willams, K., "Finite Element Analysis of Cellular Structures ," Doctoral Dissertation, University of California, Berkeley, December 1969.

23. Zienkiewicz, O.C., "The Finite Element Method in Structural and Continuum Mechanics," McGraw Hill 1967.

24. Yuille, I.M., "Shear Lag in Stiffened Plates," INA 1955.